OPEN ACCESS

ORIGINAL ARTICLE

Fatty acid ethyl ester synthase inhibition ameliorates ethanol-induced Ca^{2+}-dependent mitochondrial dysfunction and acute pancreatitis

Wei Huang,[1,2,3] David M Booth,[1] Matthew C Cane,[1] Michael Chvanov,[1,2] Muhammad A Javed,[1,2] Victoria L Elliott,[2] Jane A Armstrong,[2] Hayley Dingsdale,[1] Nicole Cash,[1] Yan Li,[2] William Greenhalf,[2] Rajarshi Mukherjee,[1,2] Bhupendra S Kaphalia,[4] Mohammed Jaffar,[5] Ole H Petersen,[6] Alexei V Tepikin,[1] Robert Sutton,[2] David N Criddle[1,2]

▶ Additional material is published online only. To view please visit the journal online (http://dx.doi.org/10.1136/gutjnl-2012-304058).

For numbered affiliations see end of article.

Correspondence to
Dr David N Criddle, Department of Cellular & Molecular Physiology/NIHR Pancreas Biomedical Research Unit, RLBUHT, Institute of Translational Medicine, University of Liverpool, Liverpool, Merseyside L693BX, UK; criddle@liv.ac.uk

WH and DMB contributed equally.

Received 1 November 2012
Revised 30 August 2013
Accepted 15 September 2013
Published Online First 25 October 2013

ABSTRACT

Objective Non-oxidative metabolism of ethanol (NOME) produces fatty acid ethyl esters (FAEEs) via carboxylester lipase (CEL) and other enzyme action implicated in mitochondrial injury and acute pancreatitis (AP). This study investigated the relative importance of oxidative and non-oxidative pathways in mitochondrial dysfunction, pancreatic damage and development of alcoholic AP, and whether deleterious effects of NOME are preventable.

Design Intracellular calcium ($[Ca^{2+}]_C$), NAD(P)H, mitochondrial membrane potential and activation of apoptotic and necrotic cell death pathways were examined in isolated pancreatic acinar cells in response to ethanol and/or palmitoleic acid (POA) in the presence or absence of 4-methylpyrazole (4-MP) to inhibit oxidative metabolism. A novel in vivo model of alcoholic AP induced by intraperitoneal administration of ethanol and POA was developed to assess the effects of manipulating alcohol metabolism.

Results Inhibition of OME with 4-MP converted predominantly transient $[Ca^{2+}]_C$ rises induced by low ethanol/POA combination to sustained elevations, with concurrent mitochondrial depolarisation, fall of NAD(P)H and cellular necrosis in vitro. All effects were prevented by 3-benzyl-6-chloro-2-pyrone (3-BCP), a CEL inhibitor. 3-BCP also significantly inhibited rises of pancreatic FAEE in vivo and ameliorated acute pancreatic damage and inflammation induced by administration of ethanol and POA to mice.

Conclusions A combination of low ethanol and fatty acid that did not exert deleterious effects per se became toxic when oxidative metabolism was inhibited. The in vitro and in vivo damage was markedly inhibited by blockade of CEL, indicating the potential for development of specific therapy for treatment of alcoholic AP via inhibition of FAEE generation.

Significance of this study

What is already known about this subject?

- Acute alcoholic pancreatitis can be a severe and life-threatening disease, which currently lacks a clear target and specific therapy.
- Both oxidative and non-oxidative ethanol metabolites have been implicated in ethanol-mediated damage of the exocrine pancreas, although their relative contributions to pancreatic toxicity remain unclear.
- Increasing evidence has implicated mitochondrial dysfunction as a key event in the pathophysiology of acute pancreatitis.
- Currently there is no convenient and reliable in vivo experimental model of alcoholic acute pancreatitis to test potential therapies.

What are the new findings?

- A new model of alcoholic acute pancreatitis has been developed.
- Promotion of non-oxidative ethanol metabolism via suppression of the oxidative pathway exacerbated ethanol-induced Ca^{2+}-dependent mitochondrial dysfunction and toxicity in vitro and acute pancreatitis in vivo.
- Non-oxidative ethanol metabolites localised to mitochondria of pancreatic acinar cells and underwent hydrolysis to release free fatty acids.
- Pharmacological inhibition of carboxylester lipase (CEL) prevented fatty acid ethyl ester formation and ameliorated in vitro exocrine pancreatic damage and in vivo acute pancreatitis induced by fat and ethanol.

INTRODUCTION

In recent decades there has been a marked elevation in alcohol consumption mirrored by a dramatic increase in the incidence of acute pancreatitis (AP). Approximately 20% of affected individuals develop extensive disease characterised by significant pancreatic necrosis and systemic inflammation, which may lead to multiple organ failure and death. Our understanding of the pathogenesis of alcoholic AP remains incomplete and currently no specific therapy exists.

The exocrine pancreas uses both oxidative and non-oxidative metabolism of ethanol (OME and NOME, respectively) to degrade alcohol, the latter combining ethanol with fatty acids to yield lipophilic fatty acid ethyl esters (FAEEs).[1] A seminal study showed that FAEEs accumulated in the pancreas of patients

To cite: Huang W, Booth DM, Cane MC, *et al*. *Gut* 2014;**63**:1313–1324.

Significance of this study

How might it impact on clinical practice in the foreseeable future?

- New insights into the underlying pathology of acute alcoholic pancreatitis reveal a specific enzyme target (CEL) that may be inhibited to ameliorate ethanol-induced injury.
- Elucidation of the molecular basis of non-oxidative ethanol metabolism mediated by CEL and inhibition by 3-benzyl-6-chloro-2-pyrone (3-BCP) will facilitate rational design of novel therapeutic compounds that may now be evaluated using a convenient and reliable experimental model of acute alcoholic pancreatitis.

following acute alcohol intoxication, in contrast to other organs commonly damaged by alcohol.[2] The balance between OME and NOME may be pivotal in determining toxic effects of excess alcohol. For example, blockade of OME by 4-methylpyrazole (4-MP) increased pancreatic FAEE levels of rats in response to ethanol, resulting in organ damage and inflammation.[3]

The generation of FAEEs occurs via diverse FAEE synthase enzymes[4] that include carboxylester lipase (CEL; E.C.3.1.1.13), also known as bile salt-activated lipase,[5] inhibited by 3-benzyl-6-chloro-2-pyrone (3-BCP).[6] CEL is synthesised by pancreatic acinar cells (PACs), stored in zymogen granules, and secreted upon hormonal stimulation.[7] Long-term ethanol feeding increased pancreatic CEL in rats,[8] while high FAEE concentrations remain in the serum of patients after ethanol ingestion,[9] persisting for up to 99 h in heavy drinkers.[10] Raised levels (>5× control) occur in the serum of patients with acute interstitial or necrotising pancreatitis.[11]

We previously demonstrated that FAEEs induced toxic sustained $[Ca^{2+}]_C$ elevations in PACs that led to necrosis.[12] Mitochondrial dysfunction was central to damage; Ca^{2+} overload caused loss of membrane potential ($\Delta\psi_M$) and consequent ATP fall, which impaired $[Ca^{2+}]_C$ homeostasis. Supply of ATP to the cell via patch-pipette inhibited development of toxic $[Ca^{2+}]_C$ elevations and necrosis induced by FAEEs[13] and bile acids.[14] Nevertheless, supply of ATP to stressed cells is unlikely to be a viable strategy for prevention of alcohol-induced toxicity in a clinical setting and alternative approaches are necessary.

This study has investigated whether manipulation of alcohol metabolic pathways may influence toxicity in vitro and the development of AP in vivo, and if inhibition of CEL with 3-BCP could prevent deleterious effects. Using molecular modelling, we demonstrate the likely mechanism of CEL-mediated FAEE generation and mode of 3-BCP inhibition. Our findings show that NOME promotion, in response to low ethanol/palmitoleic acid (POA) with concurrent OME inhibition, induced Ca^{2+}-dependent mitochondrial dysfunction and PAC necrosis. Furthermore, we have developed a novel experimental model of alcoholic AP based on the combination of ethanol and POA to induce acute exocrine pancreatic damage and systemic inflammation. Both in vitro and in vivo deleterious effects of ethanol/POA associated with promotion of NOME were ameliorated by CEL inhibition, suggesting potential for therapeutic intervention in alcoholic AP.

MATERIALS AND METHODS

Cell preparation and solutions

Isolated PACs from adult CD1 mice were prepared as previously described.[13] Experiments were performed at room temperature unless otherwise indicated. Extracellular solution contained (mM): 140 NaCl, 4.7 KCl, 1.13 $MgCl_2$, 1 $CaCl_2$, 10 D-glucose, 10 HEPES (adjusted to pH 7.35 using NaOH).

Measurements of $[Ca^{2+}]_C$, $\Delta\psi_M$ and NAD(P)H

Confocal imaging was performed using a Zeiss LSM510 system (Jena GmbH, Germany) at 35°C. Cells were loaded with Fluo 4-AM (3 μM; excitation 488 nm, emission 505–550 nm) or tetramethyl rhodamine methyl ester (TMRM, 100 nM; excitation 488 nm, emission >550 nm) to measure $[Ca^{2+}]_C$ and $\Delta\psi_M$, respectively, and mitochondrial metabolism (NAD(P)H autofluorescence; excitation 363 nm, emission 390–450 nm) assessed as described.[13] Image analysis was performed using AIM V.4.2 or Zen2009 software. Ethanol (10 mM), POA (20 μM), 4-MP (100 μM) and 3-BCP (10 μM) were applied alone or in combination for 10 min, after which the protonophore carbonyl cyanide 3-chlorophenylhydrazone (CCCP, 10 μM) was added to induce complete mitochondrial depolarisation. Measurements are expressed as changes from basal fluorescence (F/F_0 ratio, 'n' represents number of cells).

Detection of apoptotic and necrotic cell death pathway activation

Apoptotic cell death pathway activation was detected using rhodamine 110-aspartic acid amide (20 μM: excitation 488 nm, emission 505–550 nm), necrotic cell death pathway activation using propidium iodide (PI, 1 μM: excitation 488 nm, emission 630–693 nm) and total cell count with nuclear Hoechst 33342 (10 μg/mL: excitation 364 nm, emission 405–450 nm) as described.[14] Separate cell aliquots from each preparation were treated (30 min) with either (i) ethanol (10 mM), (ii) POA (20 μM), (iii) 4-MP (100 μM) or (iv) 3-BCP (10 μM) or combinations to differentially modulate OME and NOME. Counts were made of 30 separate fields from each experiment, repeated in triplicate or more.

Immunofluorescence

Intact pancreatic lobules or isolated acinar cells were fixed in 4% paraformaldehyde for 30 min, permeabilised with 0.2% Triton X-100 and blocked with 1% BSA/10% goat serum. CEL and mitochondria were localised using anti-bile salt-activated lipase antibody and mitochondrial anti-peptidyl-prolyl cis-trans isomerase antibody, respectively (both 1:200, Abcam, Cambridge UK). Secondary antibodies were conjugated with Alexa 488 or Alexa 546, used at a dilution of 1:1000. Nuclei were stained with Hoechst 33342 (10 μg/mL, Invitrogen). CEL antibody specificity was confirmed by Western blot (see online supplementary figure S2B).

Patch-clamp current recording

Patch-clamp (whole-cell configuration) was used to record Ca^{2+}-activated Cl^- currents (ICl_{Ca}) as described.[13] Patch-pipettes (2–3 MΩ) were filled with intracellular solution (mM): 140 KCl; 1.5 $MgCl_2$; 2 MgATP; 10 HEPES; 0.1 EGTA, pH 7.2. Currents were sampled at 10 KHz (EPC8 amplifier, HEKA, Lambrecht, Pfalz, Germany) with membrane voltage clamped at −30 mV. Changes of ICl_{Ca}, NAD(P)H and fluorescein (excitation 488 nm, emission 505–550 nm) were recorded, before and after exposure to POA-Fluor (20 μM: in pipette solution).

In vivo model of FAEE-AP

To establish FAEE-induced AP (FAEE-AP), adult CD1 mice received two intraperitoneal injections of ethanol (1.35 g/kg) and POA (150 mg/kg) at 1 h intervals. 200 μL normal saline was injected immediately prior to ethanol/POA injections to

avoid potential local damage by ethanol to peritoneal organs at the injection site. Control adult CD1 mice received either saline, ethanol (1.35 g/kg) or POA (150 mg/kg). In treatment groups, mice also received 10 mg/kg 4-MP or 30 mg/kg 3-BCP simultaneously with the first injection of ethanol/POA. Animals were sacrificed at 24 h after the first injection. Histological assessment of damage was performed after H&E staining of fixed pancreatic slices (5 μm thickness); 10 random fields per slide from all animal groups were graded by two independent, blinded observers according to severity and extent of oedema, inflammatory cell infiltration and acinar necrosis as previously described.[15] Further details of FAEE-AP model characterisation are included in online supplementary materials and methods.

Computational protein-ligand docking studies of POA and 3-BCP

Three-dimensional structures of ligands (POA and 3-BCP) were constructed (ChemDraw; V.11.0) and energy minimised. The X-ray crystallographic co-ordinates of human CEL (pdb 1F6W) were downloaded from RCSPB Protein Database and used for docking procedures. Molegro Virtual Docker (MVD V.3) was used to predict ligand binding mode in the protein active site. MolDock optimiser algorithms were used with a maximum of 10 runs and 10 000 iterations per ligand. A maximum of five poses were returned per ligand in which similar poses were clustered.[16] The top-ranked pose for each ligand was assigned with respect to affinity (hydrogen bond and other residue interactions, which may contribute to stability in the active site). The ligand-protein interactions were visualised using Molegro Molecular Viewer (V.2.2).

Statistical analysis

Statistical analysis of variance was performed using Origin 8.5. A value of $p<0.05$ was considered significant.

Chemicals

Fluo 4-AM, TMRM, secondary antibodies, Hoechst 33342 and R110-aspartic acid amide were purchased from Molecular Probes (Eugene, Oregon, USA). POA-Fluor was synthesised by Dr M Jaffar as described (see online supplementary methods and figure S1) and 3-BCP by Dr B S Kaphalia.[17] All other chemicals were purchased from Sigma (Gillingham, UK).

RESULTS

Inhibition of OME transforms transient $[Ca^{2+}]_C$ signals induced by ethanol and POA to sustained elevations: protective effects of 3-BCP

In PACs, application of ethanol (10 mM) with POA (20 μM) produced predominantly transient $[Ca^{2+}]_C$ elevations (32 of 52 cells, 61.5%), with sustained signals observed in only 23.1% (12 of 52 cells, figure 1A,B). The OME inhibitor 4-MP produced no or minimal effects on $[Ca^{2+}]_C$ per se, but greatly potentiated ethanol/POA action, increasing the proportion of sustained $[Ca^{2+}]_C$ elevations to 65.5% (figure 1B inset). Addition of 3-BCP (10 μM), which produced no effects on resting $[Ca^{2+}]_C$ alone (see online supplementary figure S7A), completely blocked the increase in sustained $[Ca^{2+}]_C$ elevations induced by ethanol/POA/4-MP (figure 1B). The inhibitory effects of 3-BCP were specific to ethanol/POA mediated changes, since oscillatory or sustained $[Ca^{2+}]_C$ elevations induced by 10 pM and 10 nM cholecystokinin, respectively, were unaffected (see online supplementary figure S7B,C).

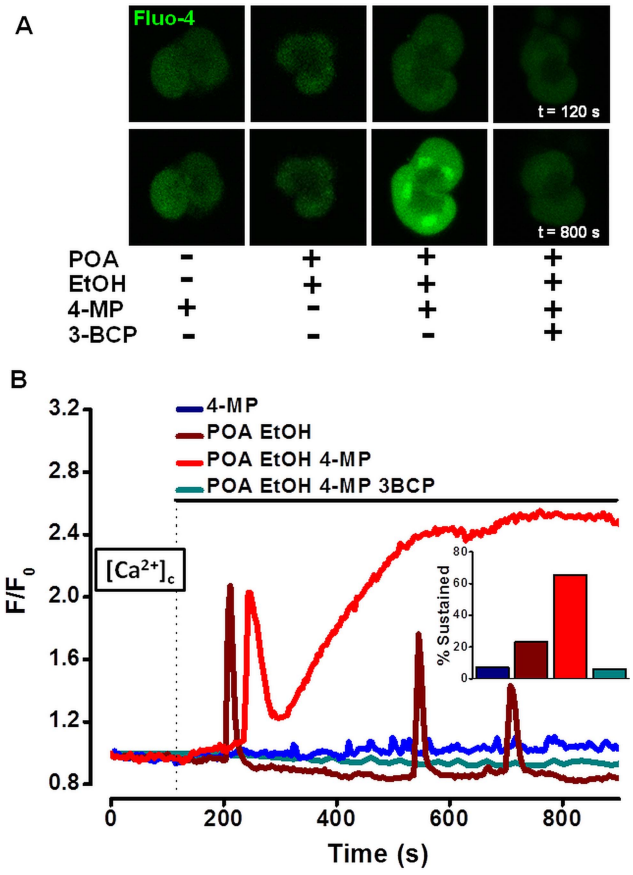

Figure 1 Effects of ethanol (EtOH), palmitoleic acid (POA), 4-methylpyrazole (4-MP) and 3-benzyl-6-chloro-2-pyrone (3-BCP) on $[Ca^{2+}]_C$ in pancreatic acinar cells. (A) Typical fluorescence images showing changes of $[Ca^{2+}]_C$ (Fluo4, *green*) before (t=120 s) and after (t=800 s) application of combinations of ethanol (10 mmol/L), POA (20 μmol/L), 4-MP (100 μmol/L) and 3-BCP (10 μmol/L). Addition of ethanol/POA/4-MP caused sustained elevation of $[Ca^{2+}]_c$ seen at 800 s. (B) Combination of ethanol/POA (*wine*) induced predominantly oscillatory increases of $[Ca^{2+}]_C$, while additional presence of 4-MP (100 μmol/L) promoted a shift towards sustained increases (*red*); 4-MP alone was without effect (*blue*). The addition of 3-BCP abolished sustained rises induced by ethanol/POA/4-MP (*cyan*). Cumulative data expressed as percentage of cells exhibiting sustained rises (inset) (F/F_0=>1.5) at 800 s (total n=159 cells).

Inhibition of OME exacerbates loss of $\Delta\psi_m$ and fall of NAD(P)H induced by EtOH and POA: protective effects of 3-BCP

A combination of ethanol (10 mM) and POA (20 μM) induced a gradual mitochondrial depolarisation in PACs. Addition of the protonophore CCCP (10 μM) after ethanol/POA caused a further loss of fluorescence as mitochondria became fully depolarised (figure 2A,B). In the additional presence of 4-MP, mitochondrial depolarisation induced by low ethanol/POA was potentiated, whereas 4-MP alone did not alter $\Delta\psi_M$. A profound reduction of NAD(P)H autofluorescence in the mitochondrial perigranular region was associated with the loss of $\Delta\psi_M$, indicative of mitochondrial inhibition (figure 2C),[14] an effect more rapid in onset when OME was inhibited (data not shown). 3-BCP (10 μM), which produced no effects on $\Delta\psi_M$ or NAD(P)H levels alone (see online supplementary figure S8B,D), completely blocked the depolarisation and fall in NAD(P)H induced by low ethanol/POA/4-MP, although further

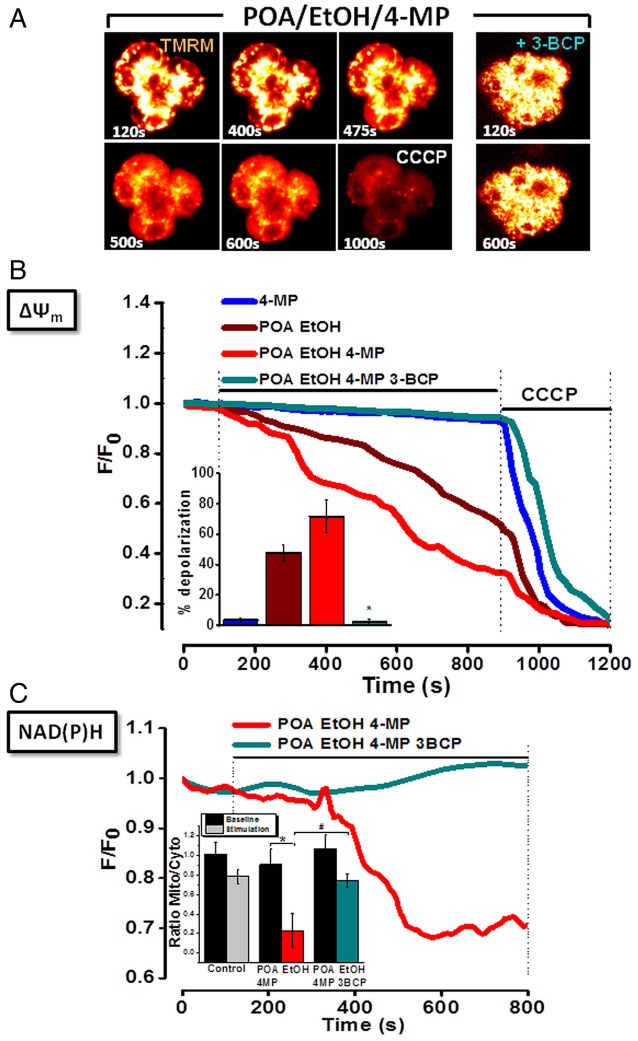

Figure 2 Effects of ethanol (EtOH), palmitoleic acid (POA), 4-methylpyrazole (4-MP) and 3-benzyl-6-chloro-2-pyrone (3-BCP) on mitochondrial membrane potential ($\Delta\psi_M$) in pancreatic acinar cells. (*A*) Typical fluorescence (*glow*) images showing progressive loss (six images, *left*) or maintenance (two images, *right*) of $\Delta\psi_M$ to ethanol/POA/4-MP combination in absence (*left*), or presence (*right*) of 3-BCP. Complete mitochondrial depolarisation induced by carbonyl cyanide 3-chlorophenylhydrazone (CCCP;10 μmol/L) is seen at 900 s. (B) Graph showing ethanol/POA-induced loss of $\Delta\psi_M$ (n=39), exacerbated by 4-MP (n=44). 4-MP alone was without effect (n=23). 3-BCP abolished effects of ethanol/POA/4-MP (n=36). Summarised data (inset) show mean % depolarisation±SE for each application. (C) Progressive loss of mitochondrial reduced nicotinamide adenine dinucleotide (phosphate) (NAD(P)H) fluorescence induced by ethanol/POA/4-MP (*red*, n=44) was abolished by 3-BCP (*cyan*, n=36). Summarised data (inset) show changes of NAD(P)H fluorescence, expressed as mean±SE in mitochondria-specific (*mito*) versus mitochondria-free (cytosolic; *cyto*) regions, at baseline (70–100 s) and during stimulation (770–800 s) (* and # $p<0.05$ compared to control).

addition of CCCP depolarised the mitochondria fully, indicating that organellar integrity had not been compromised by the ethanol/POA/4-MP combination. A partial decrease in intracellular ATP levels in response to a combination of ethanol (10 mM) and POA (20 μM) was inhibited by 3-BCP, which did not alter basal levels per se (see online supplementary figure 8E,F). Further addition of CCCP caused a maximal depletion, as shown previously.[13]

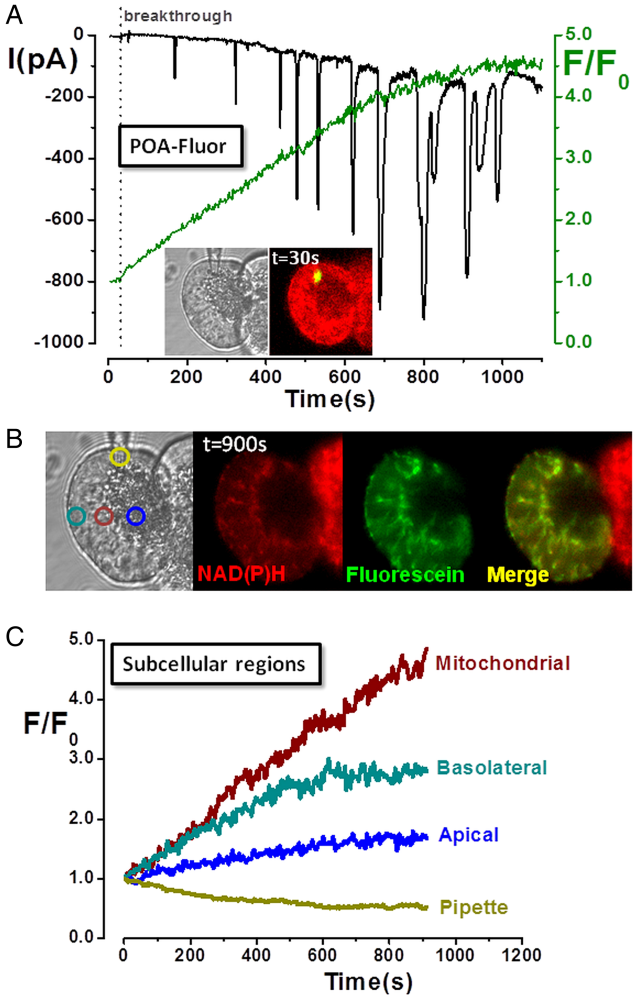

Figure 3 Mitochondrial localisation and activation of fatty acid ethyl ester probe (palmitoleic acid (POA)-Fluor) in pancreatic acinar cells. (A) Light-transmitted and fluorescent images of acinar cell doublet (*inset*) at time of membrane rupture (breakthrough) show localised fluorescence at patch-pipette tip as POA-Fluor activation by hydrolases released fluorescein. Time-dependent fluorescence rise (*green*) was associated with inward Ca^{2+}-activated Cl^- currents (ICl_{Ca}), whereas no fluorescence was detected in the adjacent cell. (B) Light-transmitted and fluorescence images, and (C) subcellular regions of interest show predominantly mitochondrial distribution of fluorescence (fluorescein: NAD(P)H co-localisation), consistent with mitochondrial probe activation. $[Ca^{2+}]_C$ levels increased over time (sustained inward ICl_{Ca} with superimposed transients), accompanied by a concomitant decrease of NAD(P)H (not seen in non-patched, adjacent cell), consistent with fatty acid-induced mitochondrial inhibition.

Mitochondrial activation of an FAEE probe induces Ca^{2+}-activated Cl^- currents (ICl_{Ca}) and mitochondrial inhibition

Previous biochemical work in cardiomyocytes suggested that FAEEs preferentially accumulate in mitochondria where they are hydrolysed to fatty acids, which uncouple oxidative phosphorylation.[18] Experiments were performed using a novel probe, POA-Fluor, composed of fluorescein linked to POA via an ester linkage, analogous to that of FAEEs. Although POA-Fluor was non-fluorescent, when administered to the PAC interior via a patch-pipette, cleavage of the probe caused a fluorescence increase as fluorescein and POA were released (figure 3A). Inward ICl_{Ca} developed following probe activation, composed of initial transients that gradually became superimposed on a

slowly developing, sustained component, indicating maintained $[Ca^{2+}]_C$ elevation. The fluorescence rise was greatest in the mitochondrial region (figure 3B,C), suggesting this was the primary site of hydrolysis, with a smaller elevation in the basolateral region, consistent with diffusion of fluorescein. In cells receiving POA-Fluor, NAD(P)H levels decreased as mitochondria were inhibited, in contrast to adjacent cells which maintained their NAD(P)H (figure 3B).

Protective effects of 3-BCP on pancreatic acinar cell fate

Simultaneous detection of apoptotic and necrotic cell death pathways in vitro showed that the NOME metabolite palmitoleic acid ethyl ester (POAEE) (50–200 μM) significantly increased cell death (figure 4A); 200 μM POAEE increased apoptosis from 0.4% (7/582 cells) to 10.8% (23/212 cells) and necrosis from 10.8% (63/582 cells) to 41.5% (88/212 cells). In contrast, application of acetaldehyde (100–200 μM) did not increase either cell death pathway above non-treated controls (figure 4A).

Ethanol (10 mM), POA (20 μM) and 4-MP (100 μM) alone produced no significant increases of either apoptotic or necrotic cell death pathway activation above control values. In contrast, the ethanol/POA/4-MP combination significantly elevated overall cell death: apoptotic cell death rose from 1.4% (16/1113 cells) to 9.5% (90/952 cells) and necrotic cell death from 4.1% (45/1113 cells) to 25.3% (247/952 cells), respectively (figure 4B). In separate experiments, application of ethanol/POA increased cell death, an effect exacerbated by inhibition of OME with 4-MP (100 μM). The CEL inhibitor 3-BCP (10 μM) significantly protected against damage induced by the ethanol/POA/4-MP combination (figure 4C).

Carboxylester lipase: localisation, formation of POAEE and inhibition by 3-BCP

Immunofluorescence showed predominantly apical, granular distribution of CEL in unstimulated isolated PACs and lobules (figure 5A,B), consistent with prior observations.[19] However, CEL was redistributed into the luminal space between acinar clusters in response to treatment with physiological cholecystokinin (10 pM), consistent with secretion (figure 5B). Such redistribution into the lumen was also apparent in pancreatic lobules from mice that received caerulein stimulation in vivo (see online supplementary figure S2A). In contrast, widespread intragranular and extragranular CEL distribution, throughout apical and basolateral regions, was observed in pancreatic lobules from mice treated with ethanol/POA to induce in vivo alcoholic AP (figure 5C). The translocation of CEL was observed in areas of tissue damage in the FAEE-AP model as early as 15 min after induction (see online supplementary figure S2C).

Computational docking studies indicated strong hydrogen bonding interactions between Ser194 (Ser-OH:HO_2C-POA; 2.75 Å) and His432 (His-N:HO_2C-POA, 2.72Å) and the carboxylic acid group of POA in the active site of CEL (figure 6A (i)). Interaction of Ser194 with the carboxylic acid moiety of POA puts it in close enough proximity (<4Å) for covalent reaction (via mechanism-based esterification) resulting in formation of a Ser-POA complex (figure 6A (ii)). The Ser-POA complex can readily react with ethanol to form POAEE (figure 6A (iii)).[20] Docking results with the CEL inhibitor 3-BCP indicated that it occupies a similar special position to the substrate allowing competition with POA for the active site (figure 6B (i)). 3-BCP is in close proximity to Ser194 (hydrogen bonding between Ser-OH…OCO-3-BCP; 2.66Å) and further stabilised by π-interactions (with Trp227 and Phe324). Moreover, the Ser194 can react covalently with 3-BCP via the C-Cl group (pathway A) or the lactone carbonyl (pathway B) to form 3-BCP-enzyme complexes in a mechanism-based inhibition/inactivation process (figure 6B (ii)).[21] Confirmation of the inhibitory action of 3-BCP on CEL was shown via a concentration-dependent reduction of the rate of

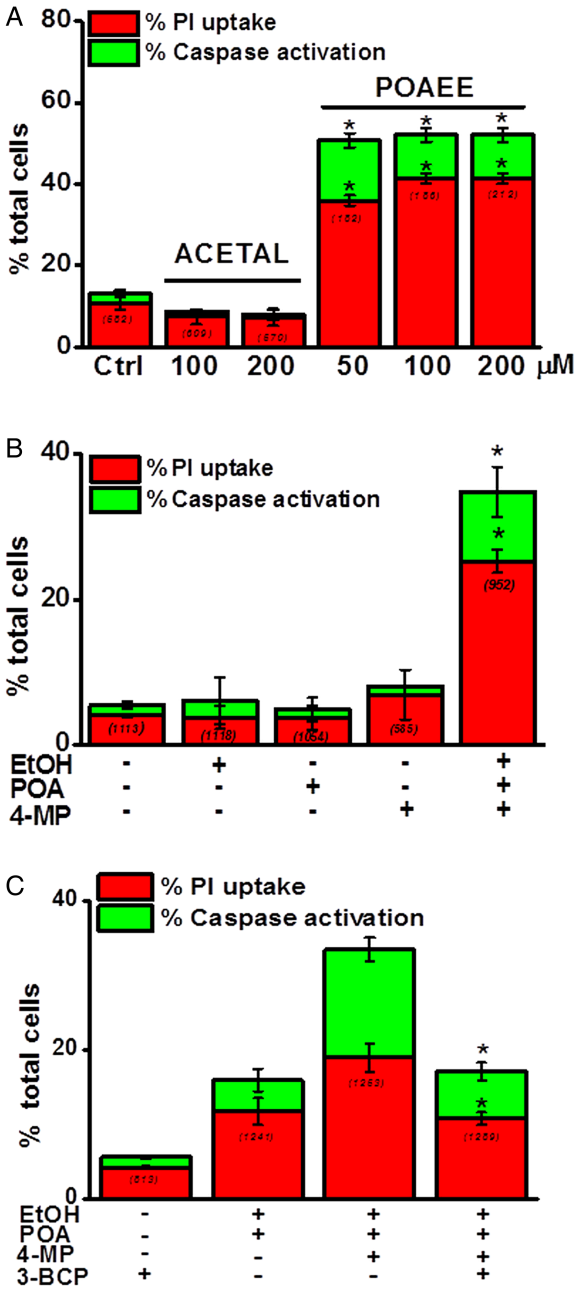

Figure 4 Importance of non-oxidative metabolism of ethanol and oxidative metabolism of ethanol in pancreatic acinar cell death. (A) Levels of apoptosis (caspase; *green*) and necrosis (PI; *red*) were increased by palmitoleic acid ethyl ester (POAEE;50–200 μmol/L) compared with controls, whereas acetaldehyde (ACETAL, 100–200 μmol/L) was without effect. (B) Ethanol (EtOH; 10 mmol/L), palmitoleic acid (POA;20 μmol/L) or 4-methylpyrazole (4-MP;100 μmol/L), applied alone, did not increase caspase activation (*green*) or PI uptake (*red*). However, a combination significantly increased apoptotic and necrotic cell death pathway activation. (C) Inhibition of carboxylester lipase with 3-benzyl-6-chloro-2-pyrone (3-BCP;10 μmol/L) reversed ethanol/POA-induced cell death precipitated by 4-MP (expressed as % total cells; mean±SE; numbers in parentheses indicate cells assessed for each experimental condition, *p<0.05 compared to control values).

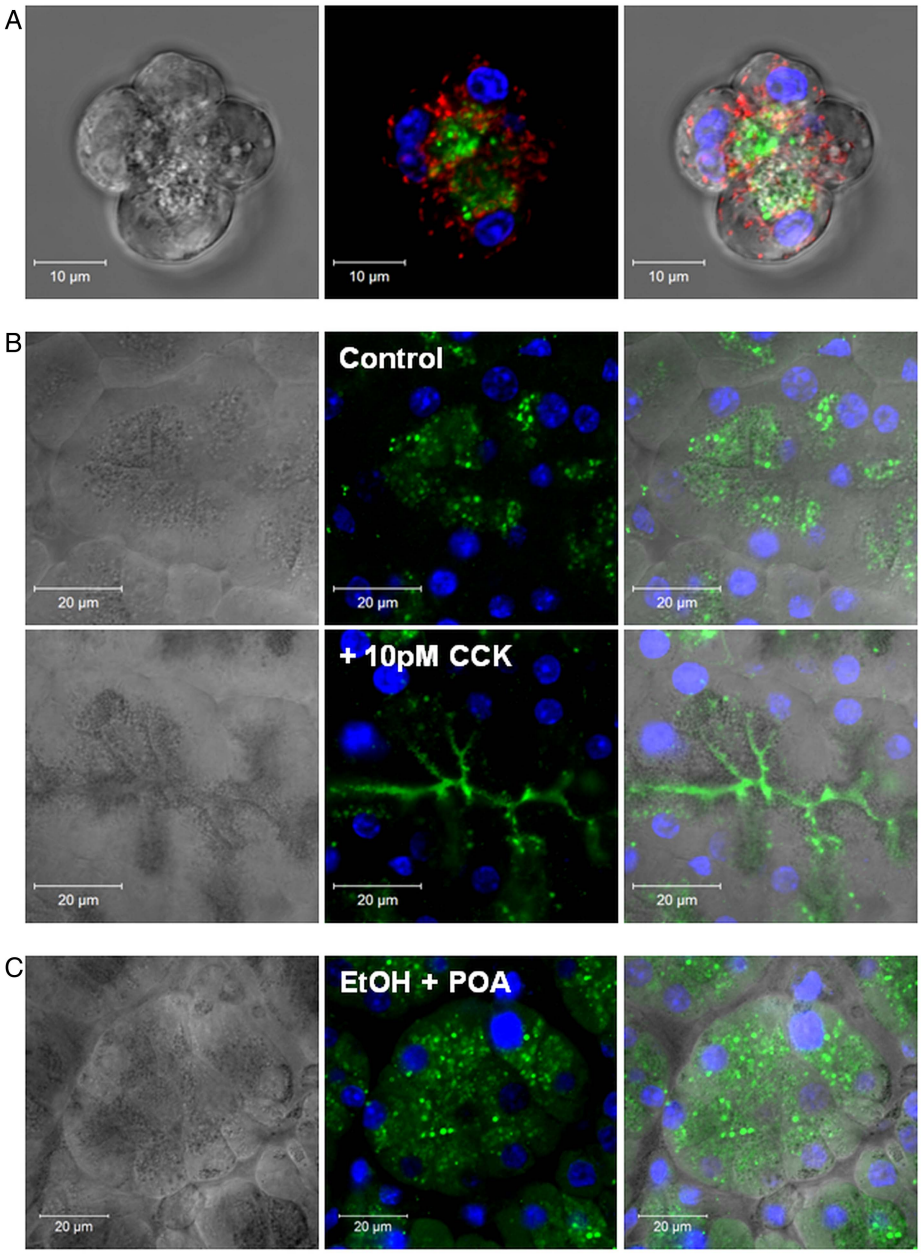

Figure 5 Localisation of carboxylester lipase (CEL) in pancreatic acinar cells and lobules. (A) Light-transmitted and fluorescent images of acinar cells showing CEL (*green*) location in the apical granular region, surrounded by peri-granular mitochondria (mitochondrial peptidyl-prolyl cis-trans isomerase: *red*). Nuclei co-stained with Hoechst 33342 (*blue*). (B) Similar distribution of CEL in unstimulated intact tissue. Treatment with physiological cholecystokinin (10 pM for 30 min) caused CEL to redistribute into the lumen between acinar clusters suggestive of secretion. (C) A diffuse intragranular and extragranular (apical and basolateral) distribution of CEL was observed in intact pancreatic lobules obtained from mice treated with ethanol/POA combination to induce alcoholic acute pancreatitis (i.p. ethanol (1.35 g/kg) and POA (150 mg/kg)).

p-nitrophenylacetate hydrolysis in isolated PACs (see online supplementary figure S5C).

Protective effects of 3-BCP in a novel in vivo model of alcoholic AP: FAEE-AP

The potential protective effects of 3-BCP were investigated in a novel in vivo model of alcoholic AP. Intraperitoneal injections of ethanol (1.35 g/kg), in combination with POA (0, 10, 20, 80 and 150 mg/kg), induced pancreatic damage observed in histological slices taken 24 h after application, with extensive acinar cell oedema, neutrophil infiltration and necrosis apparent at 80 and 150 mg/kg (figure 7A). The combination of ethanol/POA also elicited alveolar membrane thickening and inflammatory infiltration of the lung but did not damage liver, kidney or heart (figure 7B). Similarly, biochemical markers of AP, including serum amylase, pancreatic trypsin and myeloperoxidase (MPO) activity, were elevated in a dose-dependent manner by the ethanol/POA combination (figure 7C (i–iii)). The time courses of biochemical changes in the FAEE-AP model induced by ethanol and POA are shown in online supplementary materials and figure S3. In a similar manner, AP was induced by direct intraperitoneal application of POAEE, thereby bypassing the endogenous synthetic route or alternatively using oleic acid instead of POA (see online supplementary figure S4).

Application of 3-BCP (30 mg/kg) significantly reduced elevations of serum amylase, pancreatic trypsin activity and pancreatic MPO induced by ethanol/POA (figure 8A–D). Similarly, it greatly ameliorated histopathological pancreatic damage induced by ethanol/POA; overall histology score, acinar cell oedema, neutrophil infiltration and necrosis were all significantly reduced by 3-BCP (figure 9A,B (i–iv)). In contrast, ethanol or POA alone caused either a slight or no increase, respectively, in the overall histopathology score (figure 9B (i)). The mild effect of ethanol alone was due to small but significant elevations of neutrophil infiltration and oedema rather than acinar cell necrosis that remained unaltered (figure 9B (ii–iv)). Concurrent inhibition of OME by 4-MP, which by itself did not induce pancreatic damage, caused significantly greater PAC necrosis than that

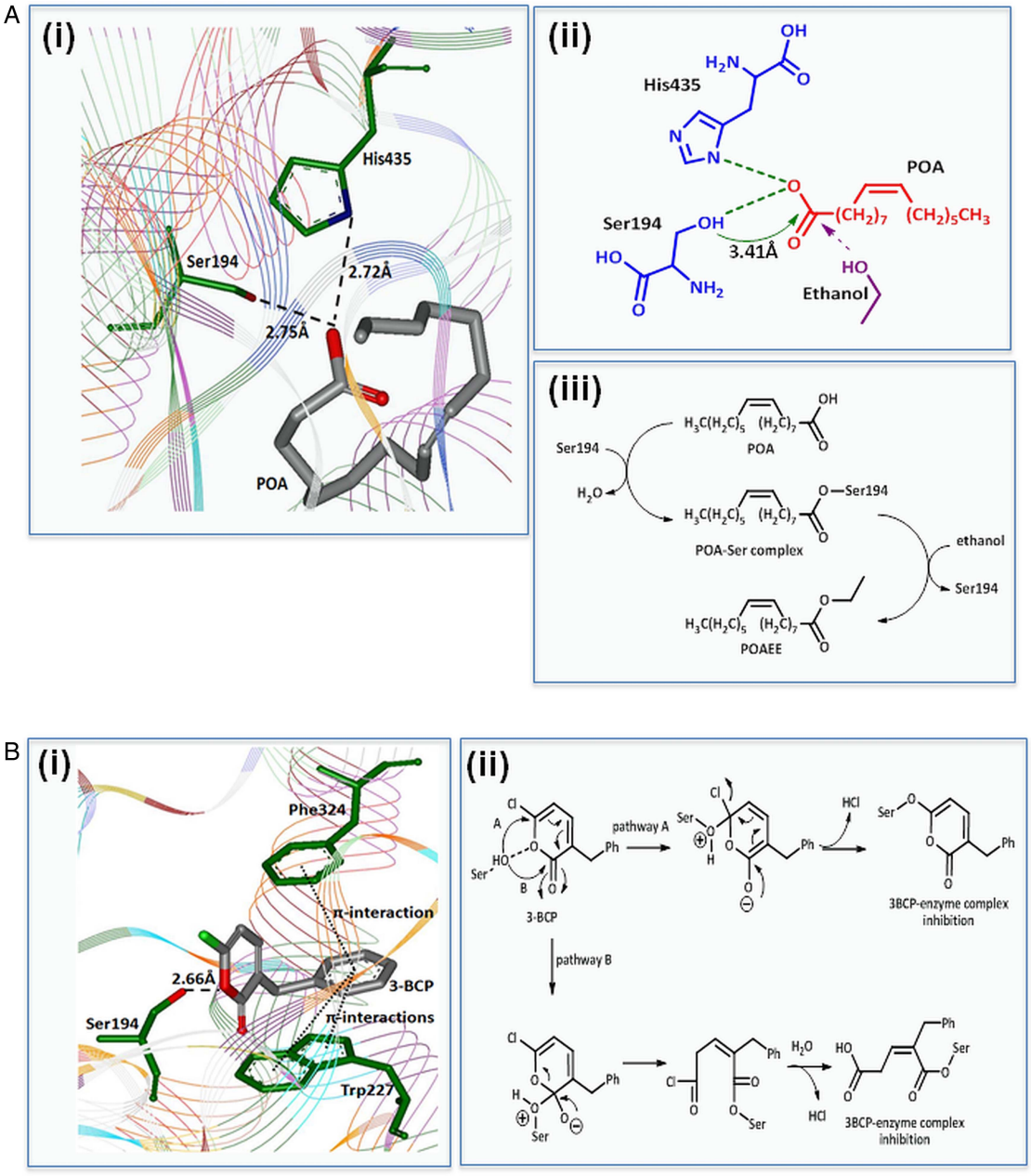

Figure 6 Proposed mechanism of fatty acid ethyl ester (FAEE) generation by carboxylester lipase (CEL) and inhibition by 3-benzyl-6-chloro-2-pyrone (3-BCP). (A) (i) Molecular docking interactions predict binding of palmitoleic acid (POA) in the active site of CEL via interaction with Ser194 and His435 residues suggesting feasibility of mechanism-based esterification. (ii) 2D representation of the binding mode of POA in the active site indicates that the Ser194 hydroxyl group can react with the POA carbonyl group to afford a POA-Ser complex; ethanol easily displaces Ser from the complex forming POA ethyl ester (POAEE). (iii) Mechanism-based esterification of POA to POAEE. (B) (i) Binding of 3-BCP in CEL active site indicates interaction with Ser194 (via hydrogen bonding), further stabilised by two π-interactions with Phe324 and Trp227. (ii) Mechanism-based reaction of 3-BCP with Ser194 residue resulting in formation of 3-BCP-enzyme complex which is inhibitory for FAEE formation.

induced by ethanol/POA alone (figure 9B (iv)); however, other parameters of AP were not significantly different (figures 8A–D and 9B (ii–iii)).

An increase in POAEE was detected in the pancreas 30 min after mice received ethanol/POA, which subsequently declined during the following hours, whereas plasma POAEE remained at control levels (see online supplementary figure S5A,B). The elevation of FAEE levels in the pancreas was significantly inhibited by 3-BCP treatment (see online supplementary figure S5A). The protective effects of 3-BCP were specific to FAEE-AP since the CEL inhibitor did not ameliorate AP induced by caerulein hyperstimulation (see online supplementary figure S6A–G).

DISCUSSION

This study has demonstrated the importance of NOME in mediating acute pancreatic toxicity and inflammation induced by alcohol, damage arising primarily from Ca^{2+}-dependent mitochondrial dysfunction in PACs. Many theories have been proposed to explain the detrimental effects of alcohol in AP,[22 23] including direct actions on Ca^{2+}-release mechanisms,[24] OME-sensitised mitochondrial dysfunction[25] and formation of toxic FAEEs.[26] The association between alcohol and fat in pancreatic damage is particularly intriguing; diets rich in corn oil and alcohol induce chronic pancreatic injury in rats.[24] Epidemiological studies suggest that high fat diets may be linked to development of acute and

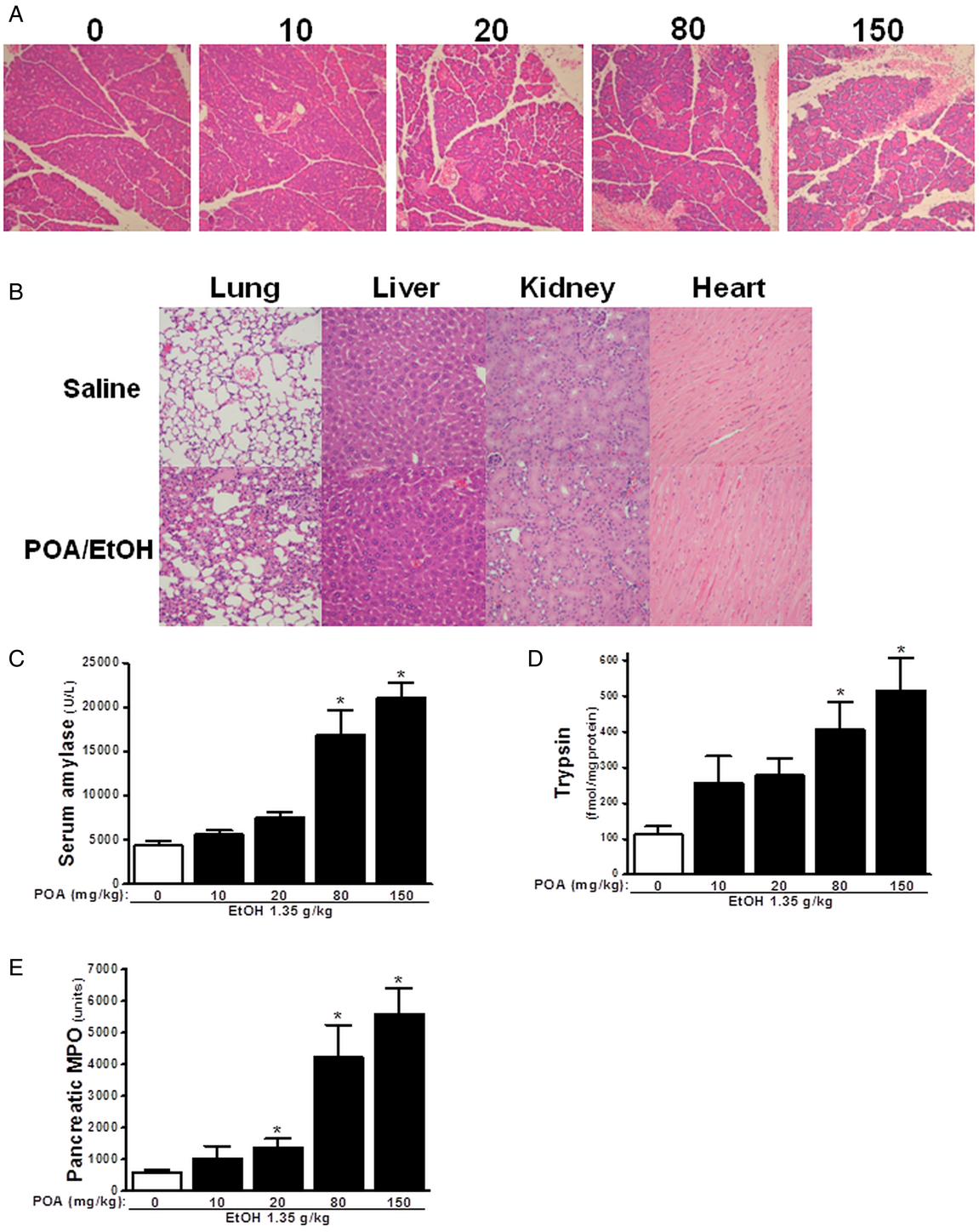

Figure 7 Features of fatty acid ethyl ester-induced acute pancreatitis induced by palmitoleic acid (POA)/ethanol. Mice received two intraperitoneal injections of ethanol (1.35 g/kg) in combination with POA at 0, 10, 20, 80 and 150 mg/kg, and mice were sacrificed 24 h after first injection. (A) Representative H&E images of histology slides from pancreas of mice treated with ethanol with POA. (B) Ethanol with POA (150 mg/kg) caused alveolar membrane thickening and inflammatory infiltration of the lung but did not induce any significant damage to liver, kidney or heart. Effects of ethanol with POA on (C) serum amylase, (D) Pancreatic trypsin activity and (E) Pancreatic myeloperoxidase activity (normalised). *p<0.05 compared to POA alone group. Values are mean±SE of 4–6 mice. Magnification: ×200.

chronic alcoholic pancreatitis,[27] while hypertriglyceridaemia is an independent risk factor for both.[28] The present data highlight the importance of NOME in mediating acute PAC damage leading to AP. It is likely that under conditions of OME inhibition, available alcohol and fatty acid from triglyceride hydrolysis are shunted towards FAEE synthesis via NOME. In anaesthetised rats in which OME was inhibited, the magnitude of FAEE production closely correlated the concentration of ethanol injected intravenously,[3] while plasma FAEE levels were raised in human subjects following 4-MP treatment.[29] Diverse FAEEs, including the unsaturated ester POAEE, are detectable in the serum of patients following ethanol ingestion.[9]

Application of exogenous POAEE greatly increased PAC death, while low level ethanol/POA, which did not cause

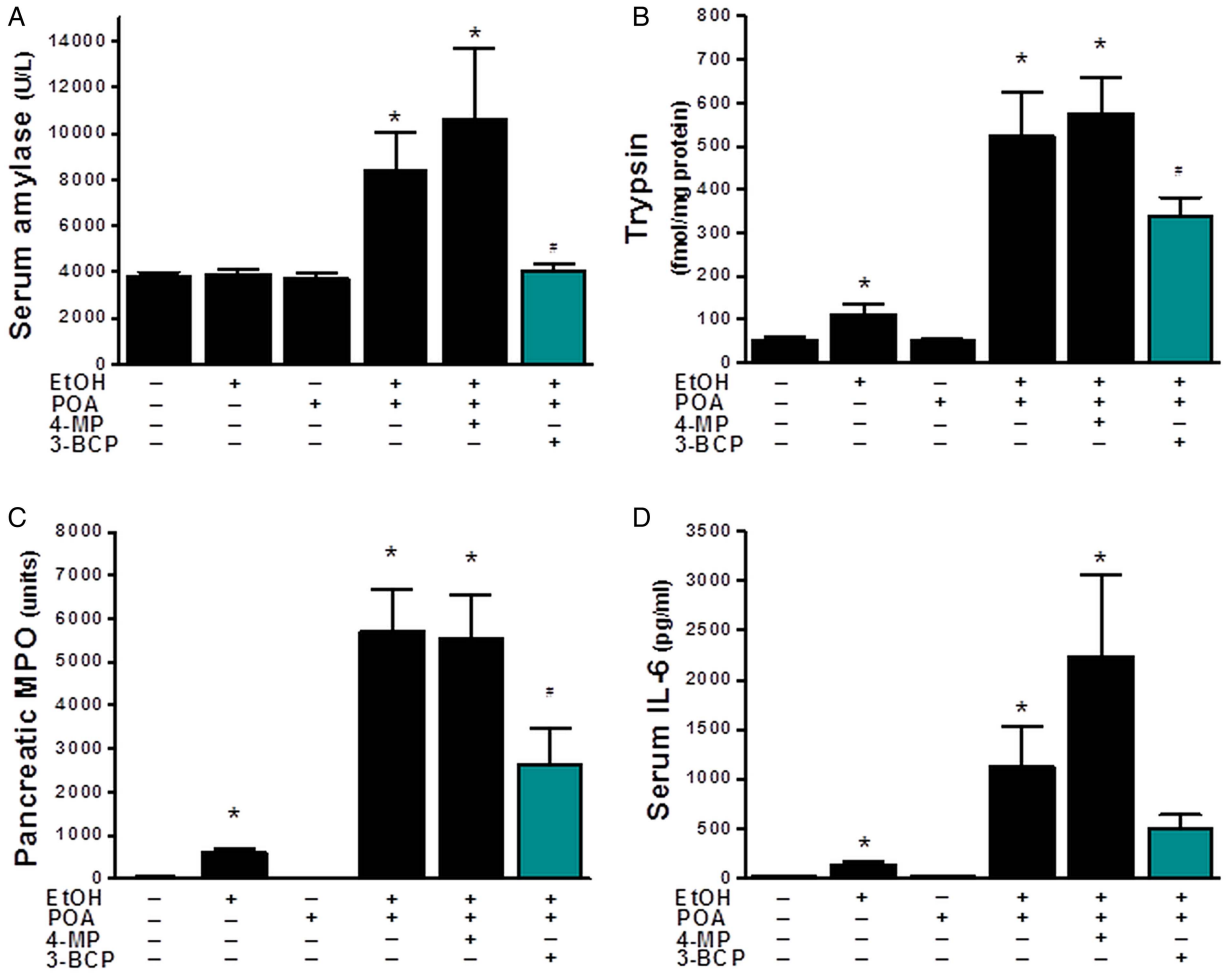

Figure 8 Protective effects of 3-benzyl-6-chloro-2-pyrone (3-BCP) on biomarkers of fatty acid ethyl ester-induced acute pancreatitis (FAEE-AP) induced by palmitoleic acid (POA)/ethanol. FAEE-AP was induced by two intraperitoneal injections of ethanol (1.35 g/kg) and POA (150 mg/kg). The effects of inhibition of oxidative metabolism of ethanol (OME) with 4-methylpyrazole (4-MP; 10 mg/kg) or non-OME with 3-BCP (30 mg/kg), given on the first injection of POA/ethanol, were assessed on (A) Serum amylase, (B) Pancreatic trypsin activity, (C) Pancreatic myeloperoxidase activity (normalised) and (D) Serum interleukin-6 (IL-6). Control mice received saline injections only. Mice were sacrificed 24 h after the first injection. *p<0.05 compared to both saline and POA controls, #p<0.05 compared to the POA/ethanol group. Values are mean±SE of 6 mice.

damage per se, became toxic when OME was inhibited. Since this effect was sensitive to 3-BCP, the most likely explanation is that FAEE generation via CEL was responsible for pancreatic injury. Importantly, in vitro damage was reflected in pathological changes in a novel murine model of alcoholic AP, a significant development in an area thus far lacking a convenient and reliable means of inducing this disease. Although the association between alcohol and AP has long been recognised, our understanding of the underlying pathophysiology has been hampered by lack of an appropriate experimental model; no reliable model of AP has been made using application of ethanol alone[30] and other agents have been required, including cholecystokinin[25 31] whose actions may be sensitised by alcohol.[25 32] In the current study, intraperitoneal injections of ethanol/POA to mice caused elevation of disease biochemical markers and development of extensive pancreatic necrosis, neutrophil infiltration and oedema. Such changes are consistent with acute damage observed in rats by intra-arterial administration of FAEEs[26] or intravenous ethanol under conditions of OME inhibition.[3] In accord with in vitro findings, 3-BCP prevented the increase of pancreatic POAEE in vivo and development of AP induced by ethanol/POA, indicating that alcohol-induced toxic effects are primarily mediated by FAEE production.

It has been suggested that OME may contribute to development of alcoholic AP via oxidative stress. For example, acute ethanol administration caused oxidative changes in rat pancreatic tissue,[33] while high concentrations of acetaldehyde in vivo damaged rat and dog pancreas.[34] In contrast to the toxic effects of POAEE, however, the OME metabolite acetaldehyde induced no increase in PAC death. This supports previous observations that acetaldehyde does not generate toxic Ca^{2+} elevations in PACs[12] and actually increased mitochondrial NAD(P)H (data not shown) that would stimulate ATP production, consistent with lack of toxicity. Furthermore, generation of reactive oxygen species in exocrine pancreas may be protective, since this promotes activation of apoptosis rather than necrosis.[14 16] Important differences between NOME and OME have been documented that support this view. For example, whereas FAEEs activated NF-κB in PACs, acetaldehyde was inhibitory,[1] while sustained elevation of acetaldehyde in ethanol-fed rats prevented hepatic inflammation and necrosis.[35]

FAEEs are reported to exert many detrimental effects on PACs, including premature activation of proteases and lipases capable of digesting subcellular structures, effects which may involve IP_3 receptor-mediated Ca^{2+} release from acidic stores[36] and increased fragility of lysosomes.[37] Previously we have shown that toxic

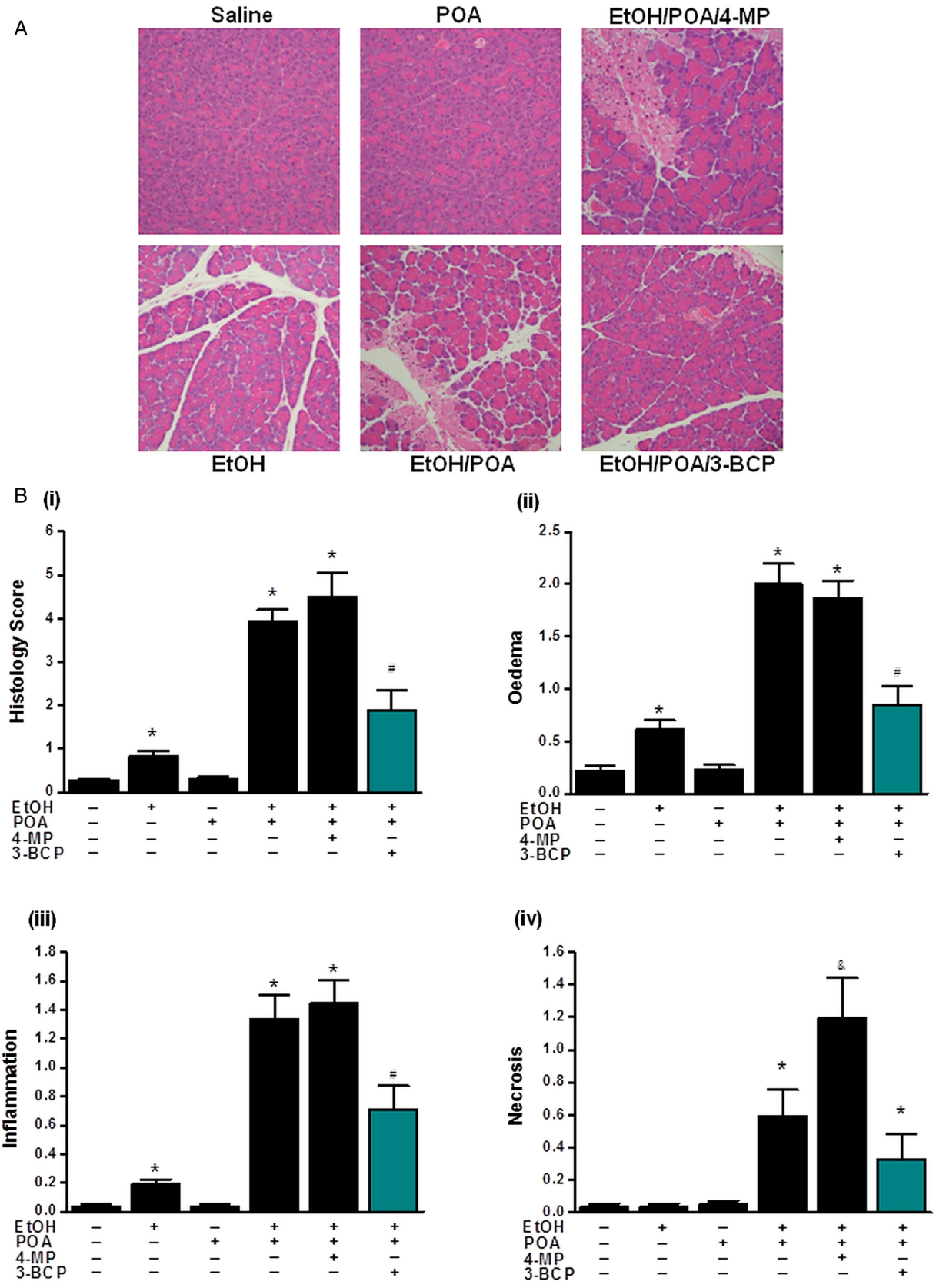

Figure 9 Protective effects 3-benzyl-6-chloro-2-pyrone (3-BCP) on histological parameters of alcoholic acute pancreatitis. (A) Representative H&E images of pancreas histology slides from treatment groups; combinations of ethanol (1.35 g/kg), palmitoleic acid (POA; 150 mg/kg), 4-methylpyrazole (4-MP; 10 mg/kg) and 3-BCP (30 mg/kg). (B)(i) Overall histopathological score and breakdown components: (ii) oedema, (iii) inflammation and (iv) necrosis. All detrimental changes induced by ethanol/POA/4-MP were significantly ameliorated by 3-BCP. (*$p<0.05$ compared to both saline and POA controls, $^{\#}p<0.05$ compared to ethanol/POA group. Values are mean±SE of 6 mice. Magnification: ×200).

effects of FAEEs occur via Ca^{2+}-dependent mitochondrial inhibition leading to a fall of ATP and necrosis.[13 38 39] In the present study, blockade of OME transformed $[Ca^{2+}]_C$ signals induced by ethanol/POA from transient rises to toxic, sustained elevations and potentiated mitochondrial inhibition. Growing evidence indicates that mitochondrial dysfunction is a core pathological feature of AP[38 40] and an absence of a functional Na^+/Ca^{2+} exchanger renders the PAC critically dependent upon ATP levels for Ca^{2+} homeostasis. Thus FAEE-induced ATP depletion would arrest Ca^{2+} extrusion via the plasmalemmal Ca^{2+}-ATPase and refilling of internal stores via the sarco-endoplasmic reticulum Ca^{2+}-ATPase, resulting in elevated $[Ca^{2+}]_C$; Ca^{2+} entry triggered by store depletion would further exacerbate mitochondrial Ca^{2+} overload. Here, use of a novel fluorescent probe indicated that FAEEs distribute to mitochondria, where breakdown occurs releasing fatty acids. This is in accord with biochemical measurements in cardiomyocytes, which demonstrated that >70% of FAEEs bound preferentially to mitochondria and underwent hydrolysis.[18] Such FAEE hydrolytic activity has been demonstrated in the human pancreas,[41] although the identity of the mitochondrial enzyme(s) responsible has yet to be clarified. Free fatty acids induce sustained $[Ca^{2+}]_C$ elevations and necrosis of PACs[12 42] and are known to uncouple mitochondria at concentrations as low as 5 μM.[18 43 44] In the present study, hydrolysis of POA-Fluor was associated with sustained elevation of $[Ca^{2+}]_C$ and loss of NAD(P)H, consistent with mitochondrial inhibition as fatty acids are released.

Diverse enzymes can synthesise FAEEs, collectively known as FAEE synthases, including CEL, triglyceride lipase, lipoprotein lipase and acyl-coenzymeA:ethanol*O*-acyltransferase.[4] These are poorly characterised, although the gene structure and cDNA sequence of human CEL has been elucidated[45] with high enzyme expression reported in pancreas.[46 47] Immunofluorescence detected CEL in the granular, apical area of PACs under basal conditions. However, stimulation with cholecystokinin in vitro or caerulein in vivo redistributed the enzyme to the luminal area in pancreatic lobes, consistent with secretion. CEL enters the secretory pathway, and in adult humans, comprises approximately 4% of protein in pancreatic juice.[48] However, pancreatic damage can release CEL into the blood[49] with increased levels reported in patients with acute interstitial or necrotising pancreatitis, leading to the proposition that CEL may constitute a sensitive marker of AP severity.[11] Furthermore, CEL redistributed outside of zymogen granules into the cytosolic compartment of necrotic PACs, with intense staining found around necrotic pancreatic lobules and in areas of fat necrosis in AP.[19] In accord, in pancreatic lobules from mice treated with ethanol/POA in vivo, there was a diffuse intragranular and extragranular distribution of CEL throughout the PACs, apparent in damaged areas as early as 15 min after application of ethanol/POA. In an alcohol-rich and fatty acid–rich environment, localised elevation of CEL would enhance production of FAEEs capable of causing extensive tissue damage. In acutely intoxicated patients, FAEEs may attain levels as high as 115 μM/L,[2] concentrations shown in the present study to elicit significant cellular necrosis.

Importantly, the damaging effects of ethanol and fat induced by promotion of NOME, both in vitro and in vivo, were significantly ameliorated by inhibition of CEL with 3-BCP, an agent previously shown to inhibit FAEE production and toxicity in cultured AR42J cells[6], and now in pancreas. Although the inhibitory action of 3-BCP has been previously documented, use of molecular modelling has now demonstrated its likely mechanism of action. Structural analysis indicates stable binding of 3-BCP into the active site of CEL, via interaction with a Ser194 residue, that would compete with fatty acids and thus inhibit ethanol-mediated fatty acid esterification required for toxic FAEE generation. Identification of critical binding features suggests that rational design of specific modulators of CEL to block FAEE production is feasible, and candidate drugs may now be tested using a convenient and reliable model of alcoholic AP.

Author affiliations
[1]Department of Cellular & Molecular Physiology, Institute of Translational Medicine, University of Liverpool, Liverpool, Merseyside, UK
[2]NIHR Liverpool Pancreas Biomedical Research Unit, RLBUHT, Institute of Translational Medicine, University of Liverpool, Liverpool, Merseyside, UK
[3]Department of Integrated Traditional Chinese and Western Medicine, Sichuan Provincial Pancreatitis Centre, West China Hospital, Sichuan University, China
[4]Department of Pathology, University of Texas Medical Branch, Galveston, Texas, USA
[5]Morvus Technology Limited, Carmarthen, UK
[6]Cardiff School of Biosciences, University of Cardiff, Cardiff, UK

Correction notice The Open Access license has been updated since published Online First.

Acknowledgements We wish to thank D Latawiec for her technical assistance.

Contributors DMB, WH, MCC, RM, MC, MAJ, VE, JA, HD, NC, YL and WG: acquisition of data; analysis and interpretation of data. BSK: material support; critical revision of the manuscript. OHP and AT: critical revision of the manuscript; obtained funding. MJ: technical and material support; acquisition of data; analysis and interpretation of data; critical revision of the manuscript. RS: study concept and design; analysis and interpretation of data; critical revision of the manuscript; obtained funding; study supervision. DNC: study concept and design; acquisition of data; analysis and interpretation of data; drafting of the manuscript; critical revision of the manuscript; obtained funding; study supervision.

Funding This study was supported by the Medical Research Council, UK (G0700167 and KO12967) and Biomedical Research Unit funding from the National Institute for Health Research; DMB was supported by an MRC Studentship; RM and MAJ were supported by Amelie Waring Clinical Research Fellowships from CORE; WH was a recipient of a UK/China Postgraduate Research Scholarships for Excellence; OHP is an MRC Professor (G19/22).

Competing interests None.

Provenance and peer review Not commissioned; externally peer reviewed.

REFERENCES

1 Gukovskaya AS, Mouria M, Gukovsky I, *et al*. Ethanol metabolism and transcription factor activation in pancreatic acinar cells in rats. *Gastroenterology* 2002;122:106–18.
2 Laposata EA, Lange LG. Presence of nonoxidative ethanol metabolism in human organs commonly damaged by ethanol abuse. *Science* 1986;231:497–9.
3 Werner J, Saghir M, Fernandez-del Castillo C, *et al*. Linkage of oxidative and nonoxidative ethanol metabolism in the pancreas and toxicity of nonoxidative ethanol metabolites for pancreatic acinar cells. *Surgery* 2001;129:736–44.
4 Laposata M. Fatty acid ethyl esters: ethanol metabolites which mediate ethanol-induced organ damage and serve as markers of ethanol intake. *Prog Lipid Res* 1998;37:307–16.
5 Best CA, Laposata M. Fatty acid ethyl esters: toxic non-oxidative metabolites of ethanol and markers of ethanol intake. *Front Biosci* 2003;8:e202–17.
6 Wu H, Bhopale KK, Ansari GA, *et al*. Ethanol-induced cytotoxicity in rat pancreatic acinar AR42J cells: role of fatty acid ethyl esters. *Alcohol Alcohol* 2008;43:1–8.
7 Lombardo D. Bile salt-dependent lipase: its pathophysiological implications. *Biochim Biophys Acta* 2001;1533:1–28.
8 Pfutzer RH, Tadic SD, Li HS, *et al*. Pancreatic cholesterol esterase, ES-10, and fatty acid ethyl ester synthase III gene expression are increased in the pancreas and liver but not in the brain or heart with long-term ethanol feeding in rats. *Pancreas* 2002;25:101–6.
9 Doyle KM, Bird DA, al-Salihi S, *et al*. Fatty acid ethyl esters are present in human serum after ethanol ingestion. *J Lipid Res* 1994;35:428–37.
10 Borucki K, Dierkes J, Wartberg J, *et al*. In heavy drinkers, fatty acid ethyl esters remain elevated for up to 99 hours. *Alcohol Clin Exp Res* 2007;31:423–7.
11 Blind PJ, Buchler M, Blackberg L, *et al*. Carboxylic ester hydrolase. A sensitive serum marker and indicator of severity of acute pancreatitis. *Int J Pancreatol* 1991;8:65–73.

12 Criddle DN, Raraty MG, Neoptolemos JP, *et al*. Ethanol toxicity in pancreatic acinar cells: mediation by nonoxidative fatty acid metabolites. *Proc Natl Acad Sci USA* 2004;101:10738–43.
13 Criddle DN, Murphy J, Fistetto G, *et al*. Fatty acid ethyl esters cause pancreatic calcium toxicity via inositol trisphosphate receptors and loss of ATP synthesis. *Gastroenterology* 2006;130:781–93.
14 Booth DM, Murphy JA, Mukherjee R, *et al*. Reactive oxygen species induced by bile acid induce apoptosis and protect against necrosis in pancreatic acinar cells. *Gastroenterology* 2011;140:2116–25.
15 Wildi S, Kleeff J, Mayerle J, *et al*. Suppression of transforming growth factor beta signalling aborts caerulein induced pancreatitis and eliminates restricted stimulation at high caerulein concentrations. *Gut* 2007;56:685–92.
16 Criddle DN, Gillies S, Baumgartner-Wilson HK, *et al*. Menadione-induced reactive oxygen species generation via redox cycling promotes apoptosis of murine pancreatic acinar cells. *J Biol Chem* 2006;281:40485–92.
17 Bailey JM, Gallo LL, Gillespie J. Inhibition of dietary cholesterol ester absorption by 3-BCP, a suicide inhibitor of cholesterol-esterase. *Biochem Soc Trans* 1995;23:408S.
18 Lange LG, Sobel BE. Mitochondrial dysfunction induced by fatty acid ethyl esters, myocardial metabolites of ethanol. *J ClinInvest* 1983;72:724–31.
19 Aho HJ, Sternby B, Kallajoki M, *et al*. Carboxyl ester lipase in human tissues and in acute pancreatitis. *Int J Pancreatol* 1989;5:123–34.
20 Tsujita T, Okuda H. The synthesis of fatty acid ethyl ester by carboxylester lipase. *Eur J Biochem* 1994;224:57–62.
21 Ringe D, Mottonen JM, Gelb MH, *et al*. X-ray diffraction analysis of the inactivation of chymotrypsin by 3-benzyl-6-chloro-2-pyrone. *Biochemistry* 1986;25:5633–8.
22 Lerch MM, Albrecht E, Ruthenburger M, *et al*. Pathophysiology of alcohol-induced pancreatitis. *Pancreas* 2003;27:291–6.
23 Apte MV, Pirola RC, Wilson JS. Mechanisms of alcoholic pancreatitis. *J Gastroenterol Hepatol* 2010;25:1816–26.
24 Gerasimenko JV, Lur G, Ferdek P, *et al*. Calmodulin protects against alcohol-induced pancreatic trypsinogen activation elicited via Ca2+ release through IP3 receptors. *Proc Natl Acad Sci USA* 2011;108:5873–8.
25 Shalbueva N, Mareninova OA, Gerloff A, *et al*. Effects of oxidative alcohol metabolism on the mitochondrial permeability transition pore and necrosis in a mouse model of alcoholic pancreatitis. *Gastroenterology* 2012;144:437–46.
26 Werner J, Laposata M, Fernandez-del Castillo C, *et al*. Pancreatic injury in rats induced by fatty acid ethyl ester, a nonoxidative metabolite of alcohol. *Gastroenterology* 1997;113:286–94.
27 Dufour MC, Adamson MD. The epidemiology of alcohol-induced pancreatitis. *Pancreas* 2003;27:286–90.
28 Yadav D, Pitchumoni CS. Issues in hyperlipidemic pancreatitis. *J Clin Gastroenterol* 2003;36:54–62.
29 Best CA, Sarkola T, Eriksson CJ, *et al*. Increased plasma fatty acid ethyl ester levels following inhibition of oxidative metabolism of ethanol by 4-methylpyrazole treatment in human subjects. *Alcohol Clin Exp Res* 2006;30:1126–31.
30 Schneider A, Whitcomb DC, Singer MV. Animal models in alcoholic pancreatitis—what can we learn? *Pancreatology* 2002;2:189–203.
31 Pandol SJ, Periskic S, Gukovsky I, *et al*. Ethanol diet increases the sensitivity of rats to pancreatitis induced by cholecystokinin octapeptide. *Gastroenterology* 1999;117:706–16.
32 Gorelick FS. Alcohol and zymogen activation in the pancreatic acinar cell. *Pancreas* 2003;27:305–10.
33 Altomare E, Grattagliano I, Vendemiale G, *et al*. Acute ethanol administration induces oxidative changes in rat pancreatic tissue. *Gut* 1996;38:742–6.
34 Nordback IH, MacGowan S, Potter JJ, *et al*. The role of acetaldehyde in the pathogenesis of acute alcoholic pancreatitis. *Ann Surg* 1991; 214:671–8.
35 Lindros KO, Jokelainen K, Nanji AA. Acetaldehyde prevents nuclear factor-kappa B activation and hepatic inflammation in ethanol-fed rats. *Lab Invest* 1999;79:799–806.
36 Gerasimenko JV, Lur G, Sherwood MW, *et al*. Pancreatic protease activation by alcohol metabolite depends on Ca2+ release via acid store IP3 receptors. *Proc Natl Acad Sci USA* 2009;106:10758–63.
37 Haber PS, Wilson JS, Apte MV, *et al*. Fatty acid ethyl esters increase rat pancreatic lysosomal fragility. *J Lab Clin Med* 1993;121:759–64.
38 Criddle DN, Gerasimenko JV, Baumgartner HK, *et al*. Calcium signalling and pancreatic cell death: apoptosis or necrosis? *Cell DeathDiffer* 2007;14:1285–94.
39 Voronina SG, Barrow SL, Simpson AW, *et al*. Dynamic changes in cytosolic and mitochondrial ATP levels in pancreatic acinar cells. *Gastroenterology* 2010;138:1976–87.
40 Booth DM, Mukherjee R, Sutton R, *et al*. Calcium and reactive oxygen species in acute pancreatitis: friend or foe? *Antioxid Redox Signal* 2011; 15:2683–98.
41 Diczfalusy MA, Bjorkhem I, Einarsson C, *et al*. Characterization of enzymes involved in formation of ethyl esters of long-chain fatty acids in humans. *J Lipid Res* 2001;42:1025–32.
42 Wang Y, Sternfeld L, Yang F, *et al*. Enhanced susceptibility to pancreatitis in severe hypertriglyceridaemic lipoprotein lipase-deficient mice and agonist-like function of pancreatic lipase in pancreatic cells. *Gut* 2009;58:422–30.
43 Jezek P, Freisleben HJ. Fatty acid binding site of the mitochondrial uncoupling protein. Demonstration of its existence by EPR spectroscopy of 5-DOXYL-stearic acid. *FEBS Lett* 1994;343:22–6.
44 Borst P, Loos JA, Christ EJ, *et al*. Uncoupling activity of long-chain fatty acids. *Biochim Biophys Acta* 1962;62:509–18.
45 Reue K, Zambaux J, Wong H, *et al*. cDNA cloning of carboxyl ester lipase from human pancreas reveals a unique proline-rich repeat unit. *J Lipid Res* 1991;32:267–76.
46 Lidberg U, Nilsson J, Stromberg K, *et al*. Genomic organization, sequence analysis, and chromosomal localization of the human carboxyl ester lipase (CEL) gene and a CEL-like (CELL) gene. *Genomics* 1992;13:630–40.
47 Kannius-Janson M, Lidberg U, Bjursell G, *et al*. The tissue-specific regulation of the carboxyl ester lipase gene in exocrine pancreas differs significantly between mouse and human. *Biochem J* 2000;351(Pt 2):367–76.
48 Lombardo D, Guy O, Figarella C. Purification and characterization of a carboxyl ester hydrolase from human pancreatic juice. *Biochim Biophys Acta* 1978;527:142–9.
49 Aleryani S, Kabakibi A, Cluette-Brown J, *et al*. Fatty acid ethyl ester synthase, an enzyme for nonoxidative ethanol metabolism, is present in serum after liver and pancreatic injury. *Clin Chem* 1996;42:24–7.

Supplementary Materials and Methods

Synthesis of POA-Fluor

To palmitoleic acid (254 mg, 1 mmol) was added oxalyl chloride (1.5 mL, excess). The mixture was stirred at room temperature for 2 h and excess oxylyl chloride was evaporated off. The crude product (palmitoleic acid chloride) was dissolved in ethyl acetate (5 mL) and fluorescein (400 mg, 1.20 mmol) was added. The mixture was stirred at room temperature for 4 h. Excess fluorescein was removed and the filtrate was purified by column chromatography (eluting with ethyl acetate) to afford the pure POA-Fluor in good yield (358mg, 63%). 1H-NMR (CDCl3): 8.01 (1H, m, Ar-H), 7.62 (2H, m, Ar-H), 7.06 (2H, m, Ar-H), 6.65 (6H, m, Ar-H), 5.35 (2H, m, HC=CH), 2.37 (2H, m, CH2), 2.02 (4H, m, 2xCH2), 1.67 (2H, m, CH2), 1.29 (16H, 8xCH2), 0.88 (3H, t, CH3). A schematic of the synthesis of POA-Fluor is shown in Supplementary Figure S1.

Acute Pancreatitis Induced by Fatty Acid Ethyl Ester

Male CD1 mice (30-35 g) were purchased from Charles River UK Ltd (Margate, UK) and housed at 23 ± 2°C under a 12-hr light/dark cycle with ad libitum access to standard laboratory chow and water. For 12 hrs before the start of the experiments, the animals were deprived of food but were allowed access to water ad libitum. Studies were conducted in compliance with the appropriate UK Home Office personal and project licence (40/3320), and with the Institutional ethical review processes of the University of Liverpool.

Initially to establish a novel alcoholic acute pancreatitis model induced by fatty acid ethyl ester (FAEE, FAEE-AP), the dose of ethanol was firstly optimised to 1.35

g/kg, which alone did not cause any obvious morphological changes in the pancreas. Palmitoleic acid ethyl ester (POAEE) was dissolved in pure ethanol to make stock solutions for injection. Mice received two intraperitoneal injection of POAEE (165 mg/kg) and ethanol (1.35 g/kg) at 1 hr interval based on the evidence that infusion of FAEE causes features of acute pancreatitis (AP) both in vivo and in vitro. To avoid local damage by ethanol to the peritoneal organs at the injection site, 200 µl of normal saline was injected immediately prior to the POAEE/ethanol injection. Analgesia was achieved by administration of 0.1 mg/kg buprenorphine hydrochloride (Temgesic, Reckitt and Coleman, Hull, England).

Induction of FAEE-AP by Fats and Ethanol

Subsequently a model was developed to more closely resemble the development of alcoholic acute pancreatitis, based on promotion of non-oxidative ethanol metabolism. Thus to demonstrate that endogenous FAEEs (i.e. synthesized from fat and ethanol by pancreatic FAEE synthase) could cause AP, oleic acid (OA, 165 mg/kg) or palmitoleic acid (POA) in combination with ethanol were also used. POA at doses of 10, 20, 80 and 150 mg/kg (equivalent molar concentration to 165 mg/kg POAEE or OA) and ethanol (1.35 kg/kg) were injected simultaneously. OA and ethanol (1.35 g/kg) were also injected simultaneously using the same regimen. Ethanol alone, and POA (150 mg/kg) alone dissolved in peanut oil were used as controls. Animals were sacrificed at various time points after the first injection for histopathology and severity marker analyses.

Induction of Caerulein (CER)-AP

In order to investigate the specificity of 3-benzyl-6-chloro-2-pyrone (3-BCP), another experimental model of acute pancreatitis was used; the caerulein (CER) hyperstimulation model [1]. Acute pancreatitis was induced in male (25-30 g) mice by 7 repeated intraperitoneal injections of CER (50 µg/kg/h) after which mice were sacrificed 12 h after first CER injection. 3-BCP (30 mg/kg) was administered at the third injection of CER whilst control animals received only saline.

Serum Amylase and IL-6 Levels

After sacrificing the mice, blood was allowed to clot naturally for 30 mins followed by centrifugation (1,500 g × 10 mins). The supernatants collected were tested at the Clinical Biochemistry Department in Royal Liverpool University Hospital, using a kinetic method [2] by Roche automated clinical chemistry analyzers (GMI, Leeds, UK). Serum IL-6 levels were tested by the ELISA method according to the instructions provided by the manufacturers (R&D, Abingdon, UK). Serum ethanol concentration was measured by an established enzymatic technique [3].

Pancreatic Water Content

The pancreata were weighed immediately following sacrifice of the mice and incubated at 90°C for 72 h. The fully dehydrated tissues were weighed again and the pancreatic water content was calculated as: wet weight-dry weight/wet weight × 100%.

Pancreatic Trypsin Activity

Pancreata were homogenised by a motorised homogeniser on ice in tissue homogenisation buffer pH 6.5, containing (in mM): MOPS 5, sucrose 250 and

magnesium sulphate 1. The resulting homogenates were centrifuged at 1500 g for 5 min, and 100 µl of each supernatant was added to a cuvette, containing peptide substrate Boc-Gln-Ala-Arg-MCA (Peptide, Osaka, Japan) dissolved in 1900 µl pH 8.0 assay buffer (in mM): Tris 50, NaCl 150, $CaCl_2$ 1 and 0.1 mg/ml bovine serum albumin. Trypsin activity was measured by fluorimetric assay using a Shimadzu RF-5000 spectrophotometer (Milton Keynes, UK). Samples were excited at 380 nm and emission collected at 440 nm [4, 5]. A standard curve was generated using purified human trypsin. Trypsin activity was expressed as fmol/mg protein or arbitrary units normalised to normal controls.

Pancreatic Myeloperoxidase Activity

Pancreatic myeloperoxidase (MPO) activity was tested by a modified method from Dawra *et al.* [6]. Myeloperoxidase activity was measured by using substrate 3,3′,5,5′-tetramethylbenzidine (TMB). Briefly, 20 µl of the supernatant was added into the assay mixture which consisted of 200 µL of phosphate buffer (100 mM, pH 5.4) with 0.5% HETAB, 20 µl TMB (20 mM in DMSO). This mixture was incubated at 37°C for 3 min, followed by the addition of 50 µL H_2O_2 (0.01%). This mixture was further incubated for 3 min. The difference of absorbance between 0 min and 3 min at 655 nm was calculated by a standard curve generated by human MPO using a plate reader. Pancreatic MPO activity was expressed as mU/mg protein or arbitrary units normalised to normal controls.

Western Blot Analysis

Protein extracted from mouse pancreatic acini was detected by Western Blot. Briefly the cells were washed with cold phosphate-buffered saline twice. The cells were

then lysated in RIPA buffer (50mM Tris-HCL pH8, 150mM NaCl, 0.5% Sodium deoxycholate, 1% Igepal CA-630 and 10% SDS). Different amounts of protein (40 µg, 20 µg, 10 µg) were sized-fractioned on 10% Mini-PROTEANR TGXTM Precast Gel (Bio-Rad Laboratories) and transferred to Trans-BlotR TurboTM Mini PVDF Transfer Packs (Bio-Rad Laboratories) using a Trans-BlotR TurboTM Transfer Starter System (Bio-Rad Laboratories). The membrane was incubated overnight at 4oC with anti-CEL (ab79131, 1:500, Abcam), and then probed with horseradish peroxidase-conjugated secondary antibodies. Anti- β-actin (1:5000, Sigma) was used as loading controls. Immunoblots were detected by enhanced chemiluminescence.

POAEE Extraction/Isolation From Plasma/Whole Pancreas

Immediately following the sacrifice of each mouse, blood was collected into an EDTA tube and the pancreas removed and placed in 1ml of hexane (placed on ice). Blood was centrifuged at 1500 x g for 10mins and the plasma layer collected. 200 µL of plasma was transferred to a fresh tube and 1ml of ice-cold acetone added, vortexed for 1min and placed on ice for 15mins. The plasma samples were then centrifuged at 600 x g and the supernatant transferred in to a fresh 15ml glass tube. The whole pancreas was homogenised in 1ml of hexane and transferred to a fresh 15ml glass tube. 2ml of ice-cold acetone was then added to the homogenate and vortexed for 1min and centrifuged at 600 x g for 10mins. The supernatant was removed and placed into a fresh 15ml glass tube. Ethyl dodecanoate (E12:0) was used as internal standard and 10 µL (1 nmole) was added to each sample. The FAEEs were then extracted by adding 2 x 4mL volumes of hexane (vortexing and centrifuging at 600 x g in between volumes) and the solvent layer transferred into a

fresh glass tube and then dried under nitrogen to 300 µL. FAEEs were then isolated using solid-phase extraction with an aminopropyl column (1mL/100mg, Chromabond, FisherScientific, UK) as described by Bernhardt et al [7]. Following which the samples were again dried under nitrogen to a final volume of 100 µL.

Quantification of POAEE

POAEE in plasma and pancreas was determined by gas chromatography–mass spectrometry (GC-MS) using a Trace Gas-Chromatograph coupled to a PolarisQ Ion-Trap mass spectrometer (ThermoScientific, Hemel Hempstead, UK) equipped with a SP-2330 capillary column (Supelcowax, Sigma, UK). The oven temperature was maintained at 160 °C for 1 min, increased to 180 °C at 3 °C/min, then further increased to 210 °C at 6 °C/min and held for 5 min. The injector and mass spectrometer were maintained at 250 and 215 °C, respectively, with a carrier gas flow rate of 1 L/min throughout. Single ion monitoring was performed, with ions m/z 55 and 236 monitored for ethyl palmitoleate (E16:1) and m/z 88 and 157 for ethyl dodecanoate (E12:0). POAEE levels in both plasma and pancreas were quantified by interpolation of the slope generated from a peak area calibration curve with increasing concentrations of E16:1 (0.5 to 10 pmole/µL) compared to a fixed concentration of the internal standard (E12:0).

Carboxylester Lipase (CEL) Inhibition Assay

CEL activity was evaluated by measuring the hydrolysis of *p*-nitrophenylacetate (PNPA), a substrate of this enzyme, as described previously [8] and the inhibitory effect of 3-BCP (1-10 µM) investigated. Isolated murine pancreatic acinar cells from CD1 mice were prepared as described earlier (Main Methods Section) and cell

pellets re-suspended in Dulbecco's modified Eagle medium containing 10 mM glucose, 2 mM L-glutamine and 2 mM sodium pyruvate. A cell count was determined using the NucleoCounter system (Chemometec) enabling seeding at 0.5 x 10^6 viable cells per 1.5 ml micro-centrifuge tube. The cells were incubated at 37^{o}C for 5 minutes with or without 3-BCP (1, 5 and 10 μM); conditions were repeated in duplicate. The cells were harvested by centrifugation at 600g for 5 minutes, washed with 0.05 M phosphate buffer (pH 7.4) and homogenised in the same buffer. The PNPA-hydrolysing activities were measured as previously described [8], using total *p*-nitrophenol formation linked to hydrolysis of cholesteryl oleate in the presence of sodium deoxycholate, and the rate of activity expressed as nmol/min/mg protein. Protein was measured using a BCA (bicinchoninic acid) assay (Pierce) with bovine serum albumin as standard.

ATP Measurement

Confocal microscopy experiments were performed on murine pancreatic acinar cells to determine changes of intracellular ATP concentrations after loading with Magnesium Green (Mg Green-AM; 4μM) for 30 min at room temperature, as previously described [9]. Decrease of intracellular ATP is seen as an increase in Mg Green fluorescence (excitation 476 nm, emission 500–550 nm) in the presence of a calcium- and magnesium-free extracellular solution.

Supplementary Figure Legends

Supplementary Figure 1. A schematic showing the synthesis and chemical structure of the palmitoleic acid-fluorescein conjugate (POA-Fluor), a novel probe for fatty acid ethyl ester activity. The fluorescein molecule is attached at the carboxylic acid moiety of POA, analogous to the ethyl ester linkage present in the non-oxidative ethanol metabolite palmitoleic acid ethyl ester (POAEE), and is released intracellularly in isolated pancreatic acinar cells via the action of hydrolase enzymes (Figure 3).

Supplementary Figure 2. Localisation of carboxylester lipase (CEL) in isolated murine pancreatic lobules. (A) Light-transmitted and fluorescent confocal images of intact pancreatic tissue obtained from mice treated with two hourly intraperitoneal injections of cerulein (0.2 µg/kg/h), which has previously been shown to stimulate secretion [10], and sacrificed 30 minutes after the second injection. CEL (*green*) is located predominantly in the lumen between the acinar clusters, indicative of secretion. Nuclei were co-stained with Hoechst 33342 (*blue*). This is in contrast to the generalised CEL distribution observed in intact pancreas obtained from mice treated with an POA/ethanol combination to induce in vivo alcoholic AP (Figure 5C). (B) Autoradiograph overlaid on a Western blot membrane showing specificity of carboxylester lipase antibody. Protein was extracted from purified murine pancreatic acini and separated by SDS-PAGE. The CEL antibody used was specific for a single band on the Western blot indicating a protein of approximately 70KDa. This is consistent with the known migration of the CEL protein and therefore indicates a high

level of specificity for the antibody. (C) Light-transmitted and fluorescent confocal images of intact pancreatic tissue obtained from control mice (*upper panels*) and mice treated with ethanol/POA combination (*lower panels*) to induce alcoholic AP (i.p. ethanol (1.35 g/kg) and POA (150 mg/kg) sacrificed at an early time-point, 15 mins after the final ethanol/POA injection. An apical CEL (*green*) distribution was observed in control animals, whereas a diffuse distribution of CEL was observed in areas of damage from intact pancreatic lobules obtained from mice treated with ethanol/POA combination. Nuclei were co-stained with Hoechst 33342 (*blue*). (Data representative of 10 samples from 4 mice (treated) and 6 samples from 4 mice (control)).

Supplementary Figure 3. Time course of FAEE-AP induced by ethanol with POA. FAEE-AP was induced by two intraperitoneal injections of ethanol (1.35 g/kg) and POA (80 mg/kg). For serum ethanol (EtOH) concentration measurements, mice were sacrificed at 1.5, 2, 3, 6 and 12 hr after the first injection, otherwise mice were sacrificed at 24 hr. Time course of (A) serum ethanol concentration, (B) Serum amylase, (C) Pancreatic water content, (D) Pancreatic trypsin activity, and (F) Pancreatic MPO activity (normalised). Values are mean ± SE of 4-6 mice.

Supplementary Figure 4. Co-administration of ethanol and palmitoleic acid ethyl ester (POAEE) or oleic acid (OA) causes AP. Fatty acid ethyl ester-induced acute pancreatitis (FAEE-AP) was induced by two intraperitoneal injections of ethanol (1.35 g/kg) with POAEE (165 mg/kg) or OA (165 mg/kg), mice were sacrificed at 2, 4, 8, 12, 24 and 48 hr after first injection. (A) Representative H&E images of histology slides from pancreas of mice treated with ethanol and POAEE. (B)

Representative H&E images of histology slides from pancreas of mice treated with OA/ethanol. Magnification, × 200.

Supplementary Figure 5. Pancreatic levels of palmitoleic acid ethyl ester (POAEE) are increased in fatty acid ethyl ester-induced acute pancreatitis (FAEE-AP) and inhibited by 3-benzyl-6-chloro-2-pyrone (3-BCP). FAEE-AP was induced by two intraperitoneal injections of ethanol (EtOH; 1.35 g/kg) with POA (50 mg/kg) and mice were sacrificed at 30 mins, 1 and 2 hrs after the first injection for POAEE measurement. (A) Graph showing increased POAEE levels in the pancreas at 30 minutes after the last ethanol/POA injection, which declined at 1 and 2 hrs but remained significantly greater than control levels. Administration of 3-BCP (30 mg/kg) significantly inhibited the increase in POAEE at 30 mins. However, plasma levels of POAEE were not significantly elevated in the FAEE-AP model consistent with a generation of FAEEs within the pancreas by carboxylester lipase (CEL). (Data are mean ± SE of 6 mice per group. *$p < 0.05$ compared to both saline and POA controls, $^{\#}p < 0.05$ compared to the POA/Ethanol group). (C) Inhibition of CEL activity by 3-BCP. The rate of CEL-induced hydrolysis of *p*-nitrophenylacetate (PNPA) in isolated murine pancreatic acinar cells was concentration-dependently inhibited by 3-BCP (1 - 10 µM). Data are expressed as the mean ± SE of 10 observations, 5 mice; *p < 0.05 compared to control).

Supplementary Figure 6. Lack of inhibitory action of 3-benzyl-6-chloro-2-pyrone (3-BCP) in a caerulein (CER) hyperstimulation model of AP. CER (50 µg/kg/h) was given as 7 intraperitoneal injections and 3-BCP (30 mg/kg) administered at the third injection of CER. Mice were sacrificed 12 h after first CER injection. Parameters of

acute pancreatitis (A) Histology score, (B) Oedema, (C) Inflammation, (D) Necrosis, (E) Serum amylase, (F) Pancreatic trypsin and (G) Pancreatic myeloperoxidase (MPO) were not significantly different between 3-BCP-treated (*cyan*) and control (*black*) groups (Data are mean ± SE of 4 mice per group).

Supplementary Figure 7. Effects of 3-benzyl-6-chloro-2-pyrone (3-BCP) and extracellular Ca^{2+} removal on $[Ca^{2+}]_C$ signals in murine pancreatic acinar cells. Typical traces showing the effects of 3-BCP (10 μmol/L) on (A) basal $[Ca^{2+}]_C$ (n = 39), (B) oscillatory rises of $[Ca^{2+}]_C$ induced by cholecystokinin (CCK; 10 pmol/L) (n = 12), (C) sustained rise of $[Ca^{2+}]_C$ induced by cholecystokinin (10 nmol/L) (n = 32), (D) sustained rise of $[Ca^{2+}]_C$ induced by palmitoleic acid (POA; 100 μmol/L) (n = 7), (E) oscillatory rises of $[Ca^{2+}]_C$ induced by POA/ethanol combination (POA; 20 μmol/L and EtOH 10 mmol/L) (n = 7), and the effects of extracellular Ca^{2+} removal on (F) oscillatory (*grey;* n = 8) and sustained (*black;* n = 3) rises of $[Ca^{2+}]_C$ induced by POA/ethanol combination (POA; 20 μmol/L and EtOH 10 mmol/L), and (G) sustained rise of $[Ca^{2+}]_C$ induced by POA/ethanol combination with 4-methylpyrazole (4-MP; 100 μmol/L) (n = 11).

Supplementary Figure 8. Protective effects of 3-benzyl-6-chloro-2-pyrone (3-BCP) on POA/ethanol-induced changes of mitochondrial membrane potential ($\Delta\psi_M$), reduced nicotinamide adenine dinucleotide (phosphate) (NAD(P)H) and adenosine triphosphate (ATP) in murine pancreatic acinar cells. The effects of 3-BCP (10 μmol/L, *cyan*) on POA/ethanol-induced (*wine*) decreases of (A) $\Delta\psi_M$ and (C) NAD(P)H (n = 11) and 3-BCP alone in control experiments (B and D, respectively) (n = 9). (Values are mean ± SE). Typical traces showing the inhibitory effects of 3-BCP

(10 µmol/L) on POA/ethanol-induced increases of Magnesium Green fluorescence, reflecting a decrease of intracellular ATP concentration (E; n = 23), with no effect in control experiments in the absence of POA/ethanol (F; n = 23). Addition of the protonophore carbonyl cyanide 3-chlorophenylhydrazone (CCCP; 10 µmol/L) was used to cause a maximal effect as previously described [9].

REFERENCES

1 Saluja AK, Lerch MM, Phillips PA, *et al.* Why Does Pancreatic Overstimulation Cause Pancreatitis? *AnnuRevPhysiol* 2006.

2 Lorentz K. Approved recommendation on IFCC methods for the measurement of catalytic concentration of enzymes. Part 9. IFCC method for alpha-amylase (1,4-alpha-D-glucan 4-glucanohydrolase, EC 3.2.1.1). International Federation of Clinical Chemistry and Laboratory Medicine (IFCC). Committee on Enzymes. *Clin Chem Lab Med* 1998;**36**:185-203.

3 Bucher T, Redetzki H. [Specific photometric determination of ethyl alcohol based on an enzymatic reaction]. *Klin Wochenschr* 1951;**29**:615-6.

4 Nathan JD, Romac J, Peng RY, *et al.* Transgenic expression of pancreatic secretory trypsin inhibitor-I ameliorates secretagogue-induced pancreatitis in mice. *Gastroenterology* 2005;**128**:717-27.

5 Kawabata S, Miura T, Morita T, *et al.* Highly sensitive peptide-4-methylcoumaryl-7-amide substrates for blood-clotting proteases and trypsin. *European journal of biochemistry / FEBS* 1988;**172**:17-25.

6 Dawra R, Ku YS, Sharif R, *et al.* An improved method for extracting myeloperoxidase and determining its activity in the pancreas and lungs during pancreatitis. *Pancreas* 2008;**37**:62-8.

7 Bernhardt TG, Cannistraro PA, Bird DA, *et al.* Purification of fatty acid ethyl esters by solid-phase extraction and high-performance liquid chromatography. *J Chromatogr B Biomed Appl* 1996;**675**:189-96.

8 Kaphalia BS, Mericle KA, Ansari GA. Mechanism of differential inhibition of hepatic and pancreatic fatty acid ethyl ester synthase by inhibitors of serine-esterases: in vitro and cell culture studies. *ToxicolApplPharmacol* 2004;**200**:7-15.

9 Criddle DN, Murphy J, Fistetto G, *et al.* Fatty Acid Ethyl Esters Cause Pancreatic Calcium Toxicity via Inositol Trisphosphate Receptors and Loss of ATP Synthesis. *Gastroenterology* 2006;**130**:781-93.

10 Saluja AK, Saluja M, Printz H, *et al.* Experimental pancreatitis is mediated by low-affinity cholecystokinin receptors that inhibit digestive enzyme secretion. *Proc Natl Acad Sci U S A* 1989;**86**:8968-71.

Figure S1

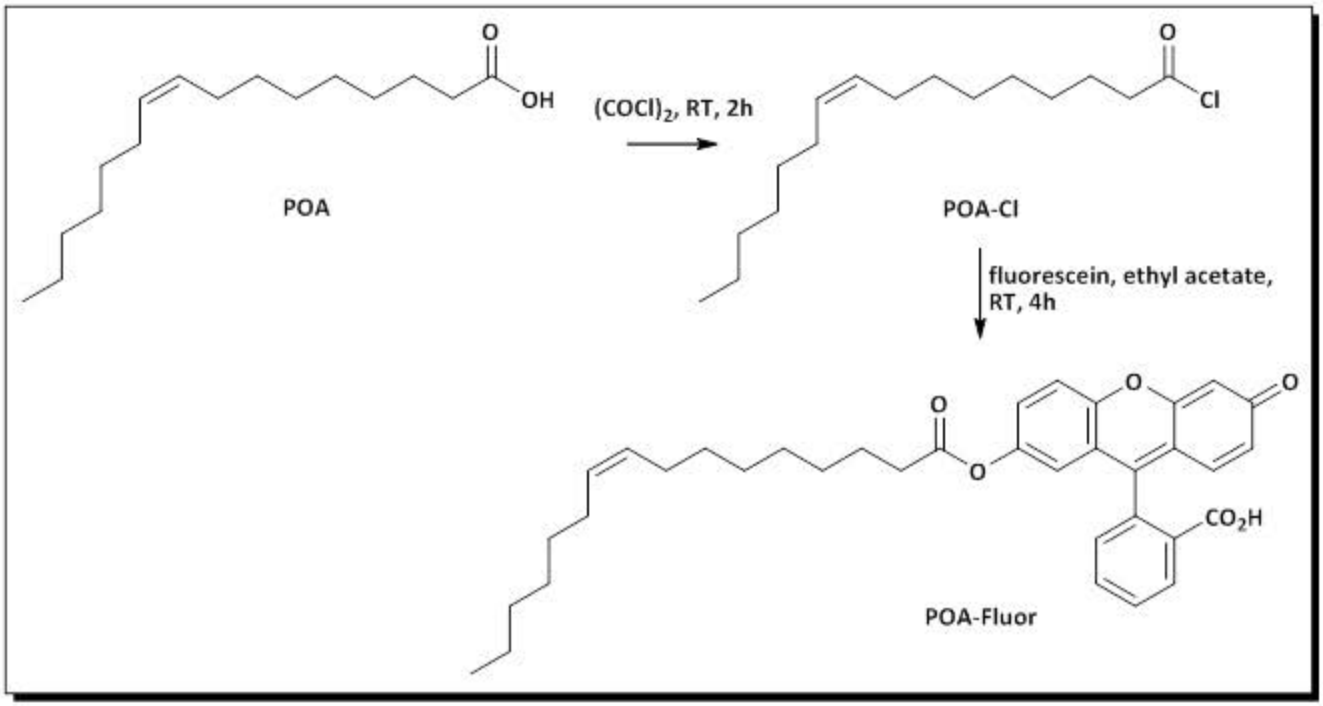
O
OH
POA
(COCl)2, RT, 2h
O
Cl
POA-Cl
fluorescein, ethyl acetate,
RT, 4h
O
O
O
O
O
CO2H
POA-Fluor

Figure S2

A

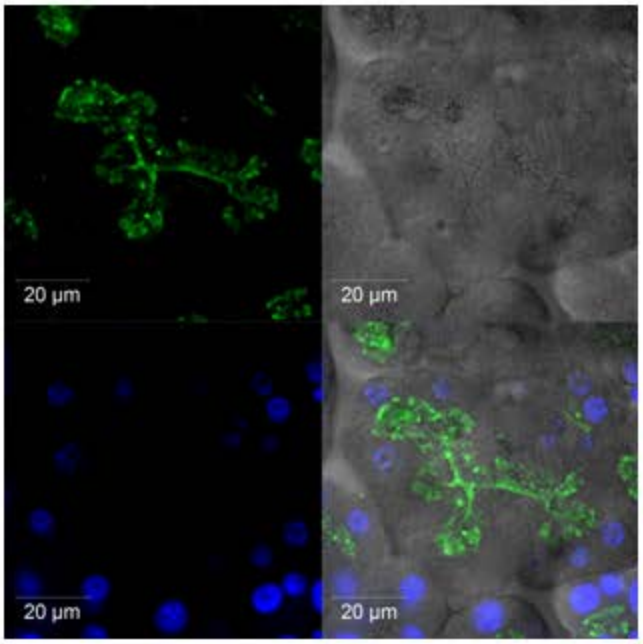

B

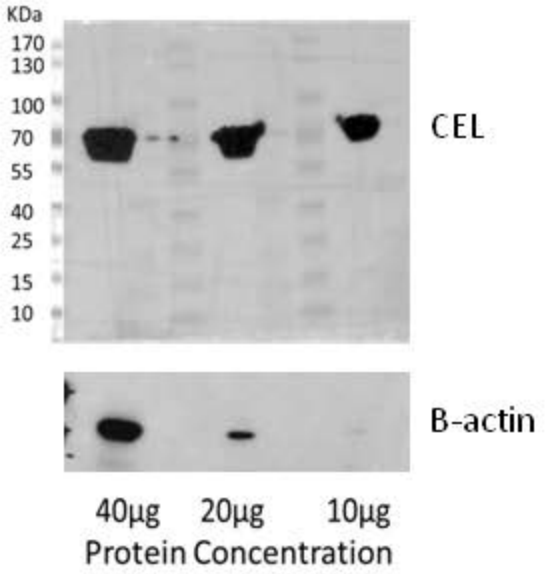

C

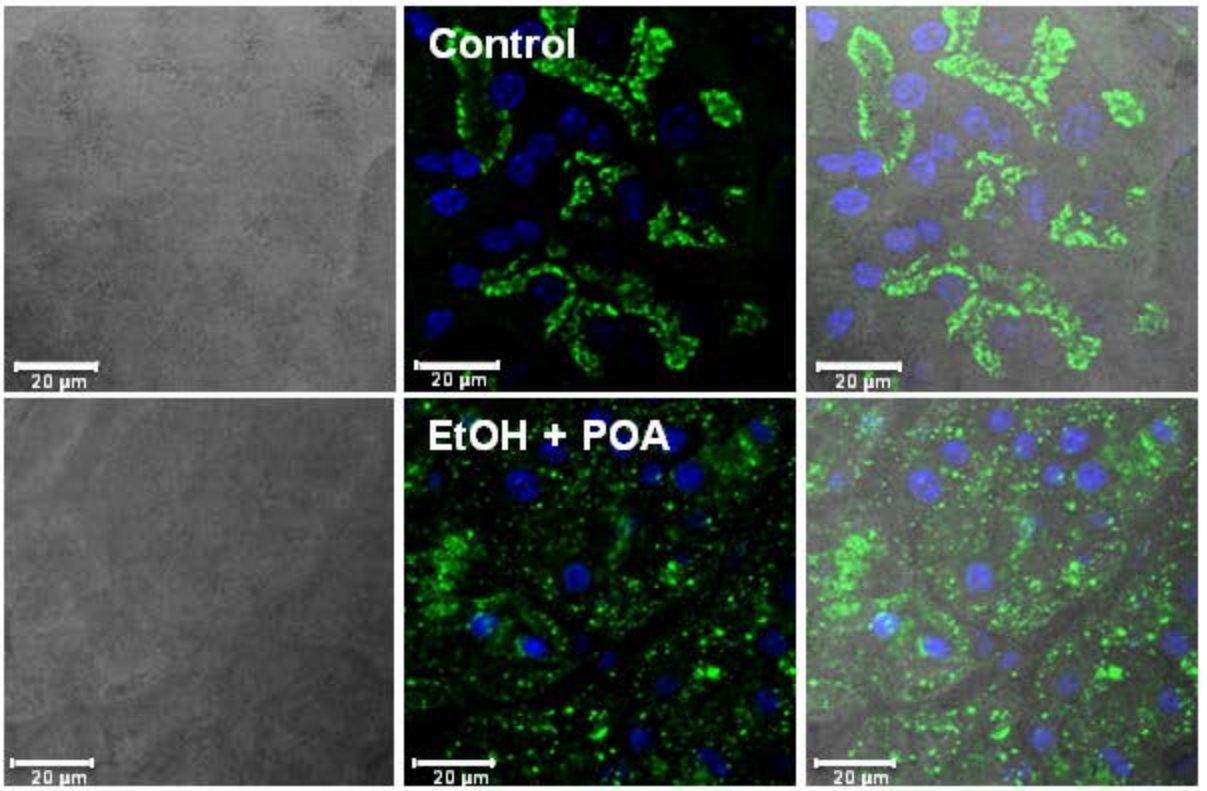

Figure S3

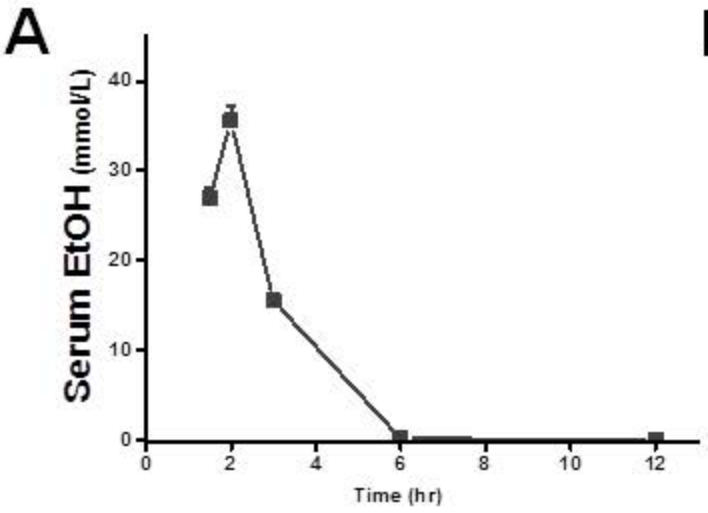
A
Serum EtOH (mmol/L)
0
10
20
30
40
0
2
4
6
8
10
12
Time (hr)

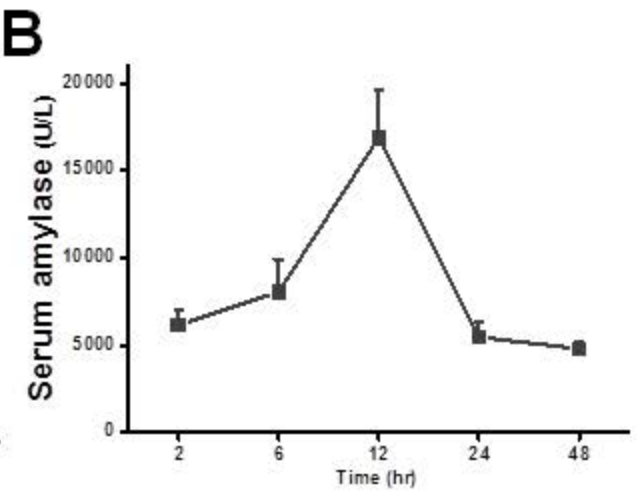
B
Serum amylase (U/L)
0
5000
10000
15000
20000
2
6
12
24
48
Time (hr)

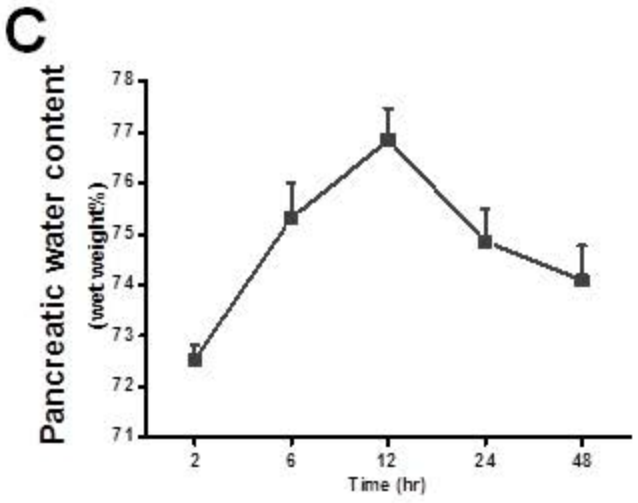
C
Pancreatic water content
(wet weight%)
71
72
73
74
75
76
77
78
2
6
12
24
48
Time (hr)

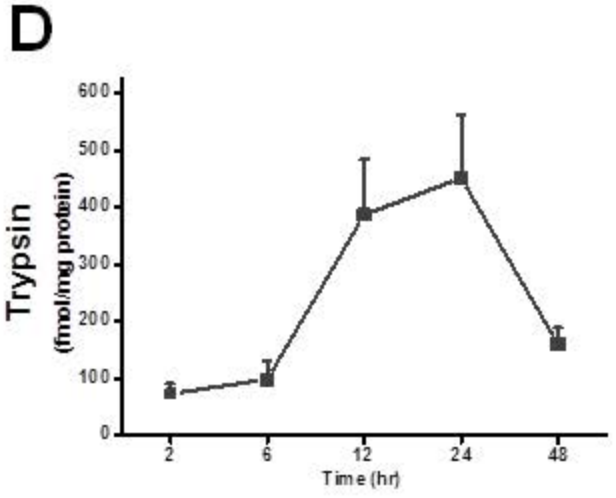
D
Trypsin
(fmol/mg protein)
0
100
200
300
400
500
600
2
6
12
24
48
Time (hr)

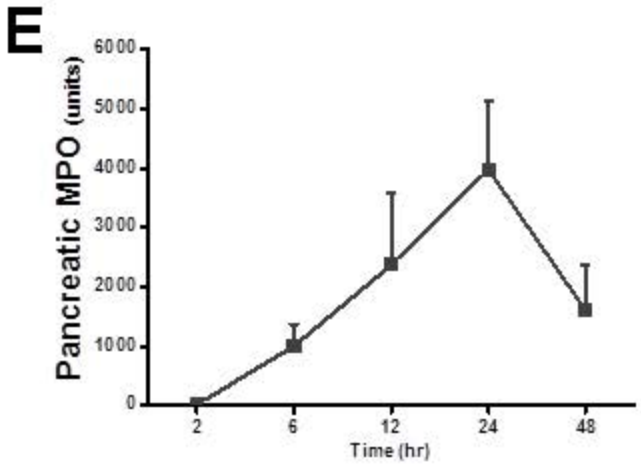
E
Pancreatic MPO (units)
0
1000
2000
3000
4000
5000
6000
2
6
12
24
48
Time (hr)

Figure S4

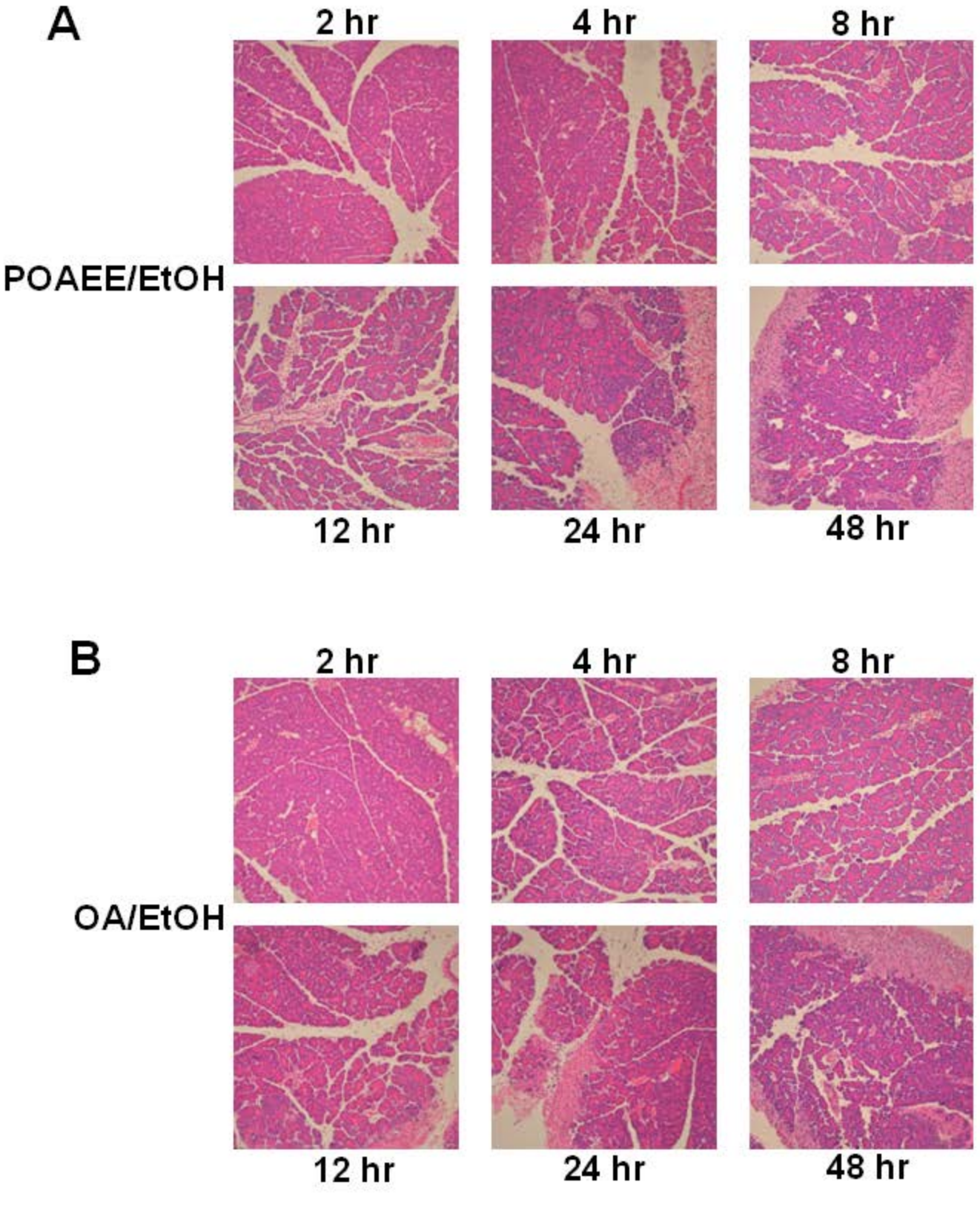
A
2 hr
4 hr
8 hr
POAEE/EtOH
12 hr
24 hr
48 hr
B
2 hr
4 hr
8 hr
OA/EtOH
12 hr
24 hr
48 hr

Figure S5

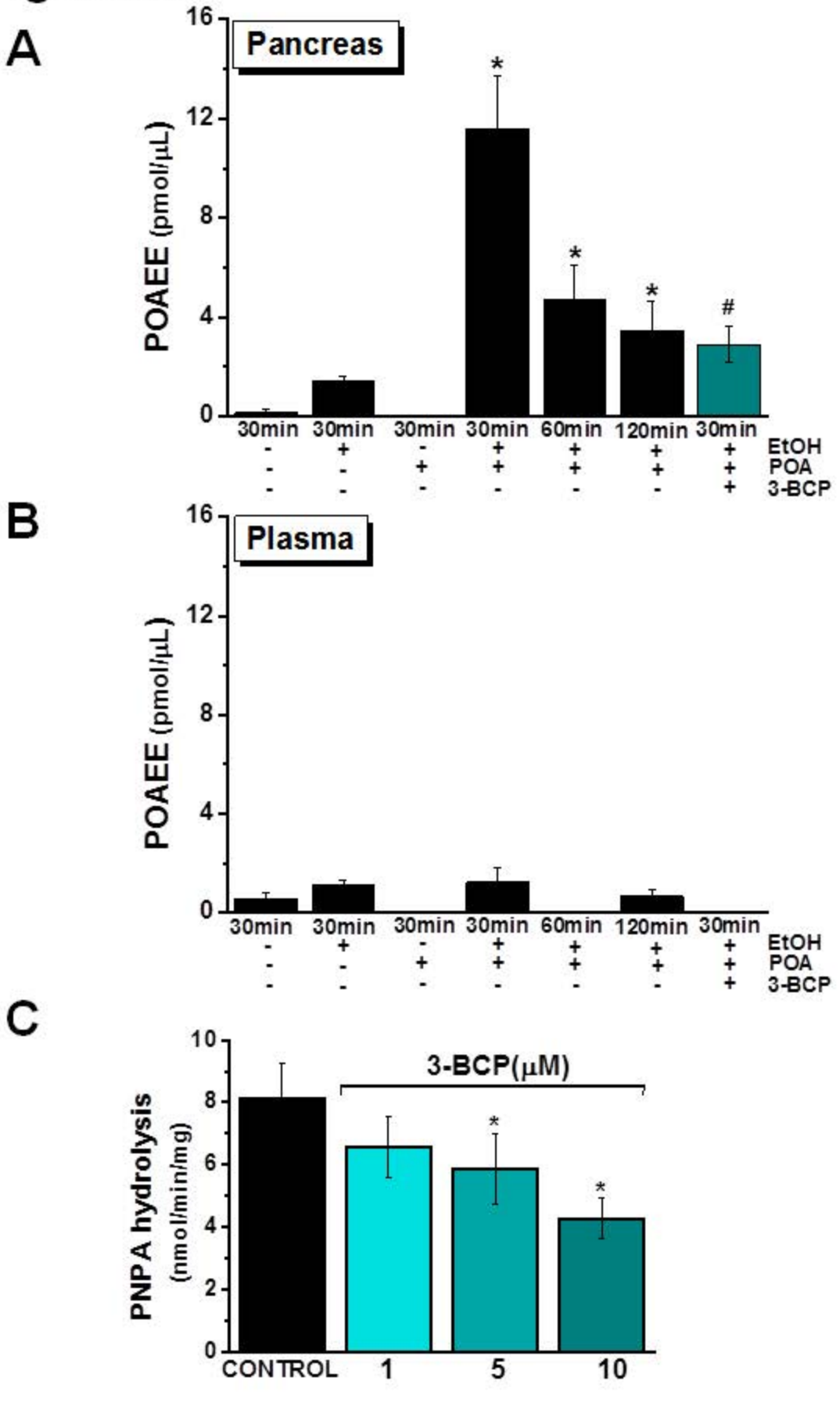
A
Pancreas
POAE (pmol/μL)
16
12
8
4
0
*
*
*
#
30min 30min 30min 30min 60min 120min 30min
EtOH - + - + + + +
POA - - + + + + +
3-BCP - - - - - - +
B
Plasma
POAE (pmol/μL)
16
12
8
4
0
30min 30min 30min 30min 60min 120min 30min
EtOH - + - + + + +
POA - - + + + + +
3-BCP - - - - - - +
C
PNPA hydrolysis (nmol/min/mg)
10
8
6
4
2
0
3-BCP(μM)
*
*
CONTROL 1 5 10

Figure S6

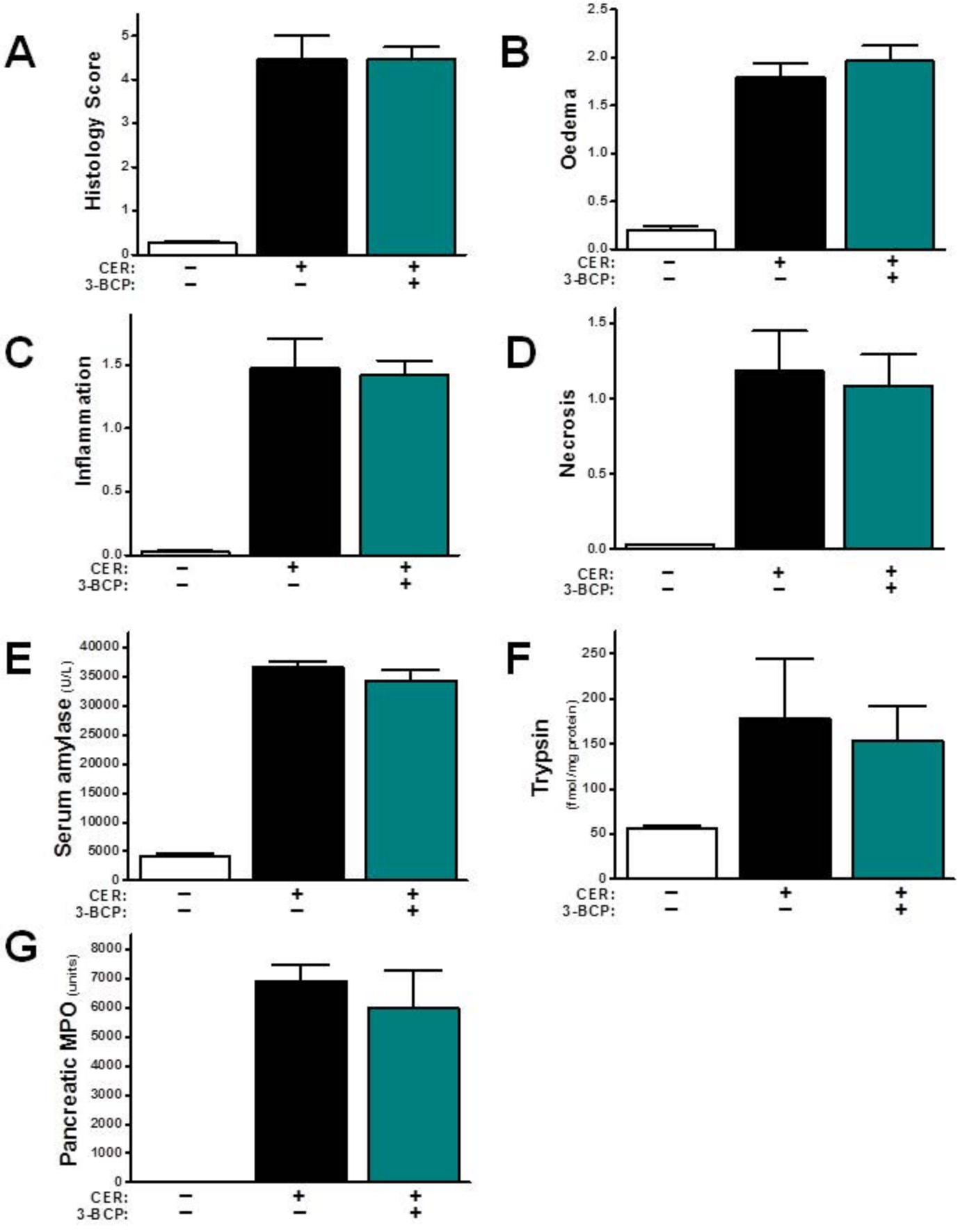
A
Histology Score
0
1
2
3
4
5
CER: – + +
3-BCP: – – +
B
Oedema
0.0
0.5
1.0
1.5
2.0
2.5
CER: – + +
3-BCP: – – +
C
Inflammation
0.0
0.5
1.0
1.5
CER: – + +
3-BCP: – – +
D
Necrosis
0.0
0.5
1.0
1.5
CER: – + +
3-BCP: – – +
E
Serum amylase (U/L)
0
5000
10000
15000
20000
25000
30000
35000
40000
CER: – + +
3-BCP: – – +
F
Trypsin
(fmol/mg protein)
0
50
100
150
200
250
CER: – + +
3-BCP: – – +
G
Pancreatic MPO (units)
0
1000
2000
3000
4000
5000
6000
7000
8000
CER: – + +
3-BCP: – – +

Figure S7

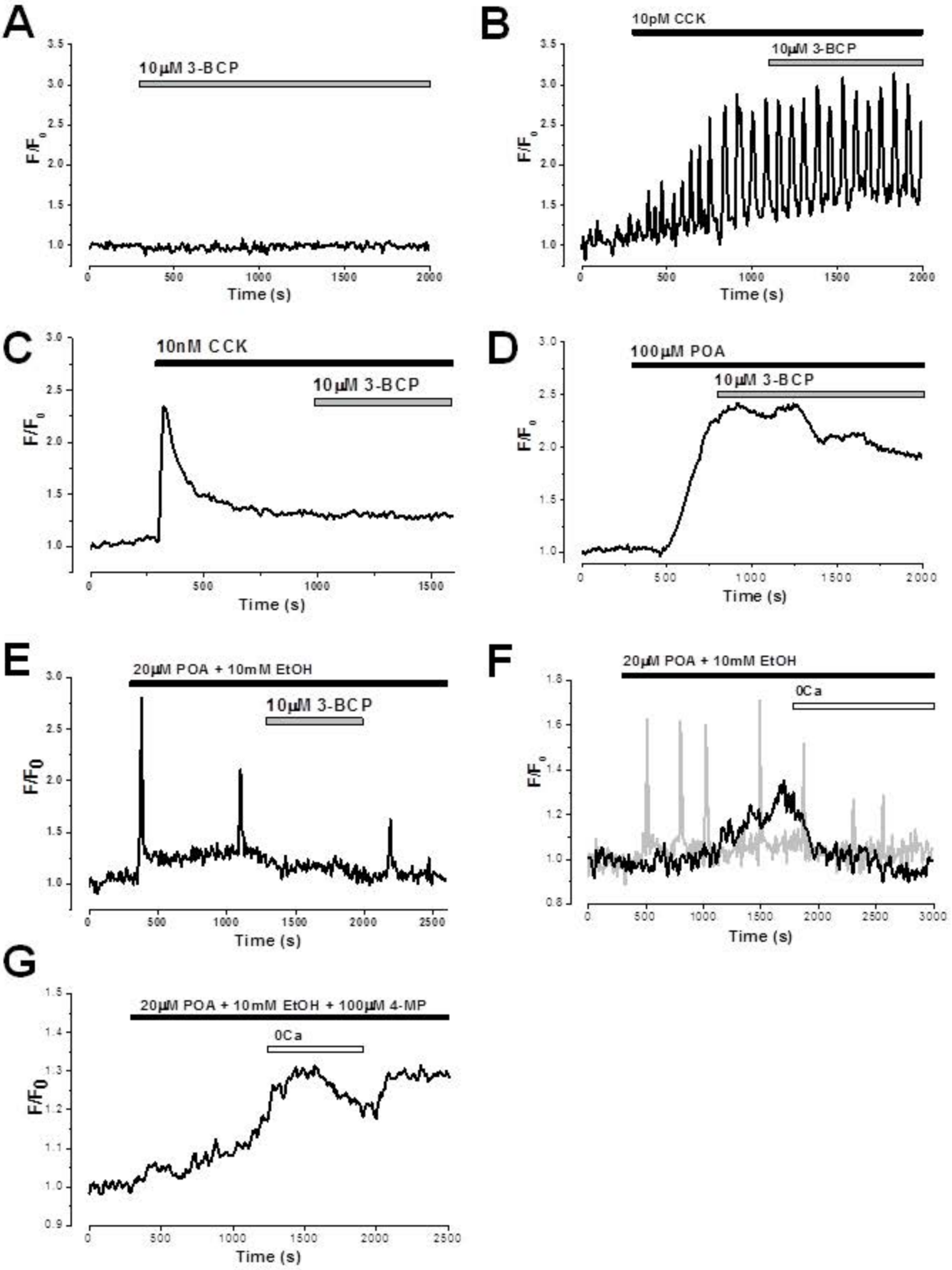
A
10μM 3-BCP
F/F0
Time (s)
B
10pM CCK
10μM 3-BCP
F/F0
Time (s)
C
10nM CCK
10μM 3-BCP
F/F0
Time (s)
D
100μM POA
10μM 3-BCP
F/F0
Time (s)
E
20μM POA + 10mM EtOH
10μM 3-BCP
F/F0
Time (s)
F
20μM POA + 10mM EtOH
0Ca
F/F0
Time (s)
G
20μM POA + 10mM EtOH + 100μM 4-MP
0Ca
F/F0
Time (s)

Figure S8

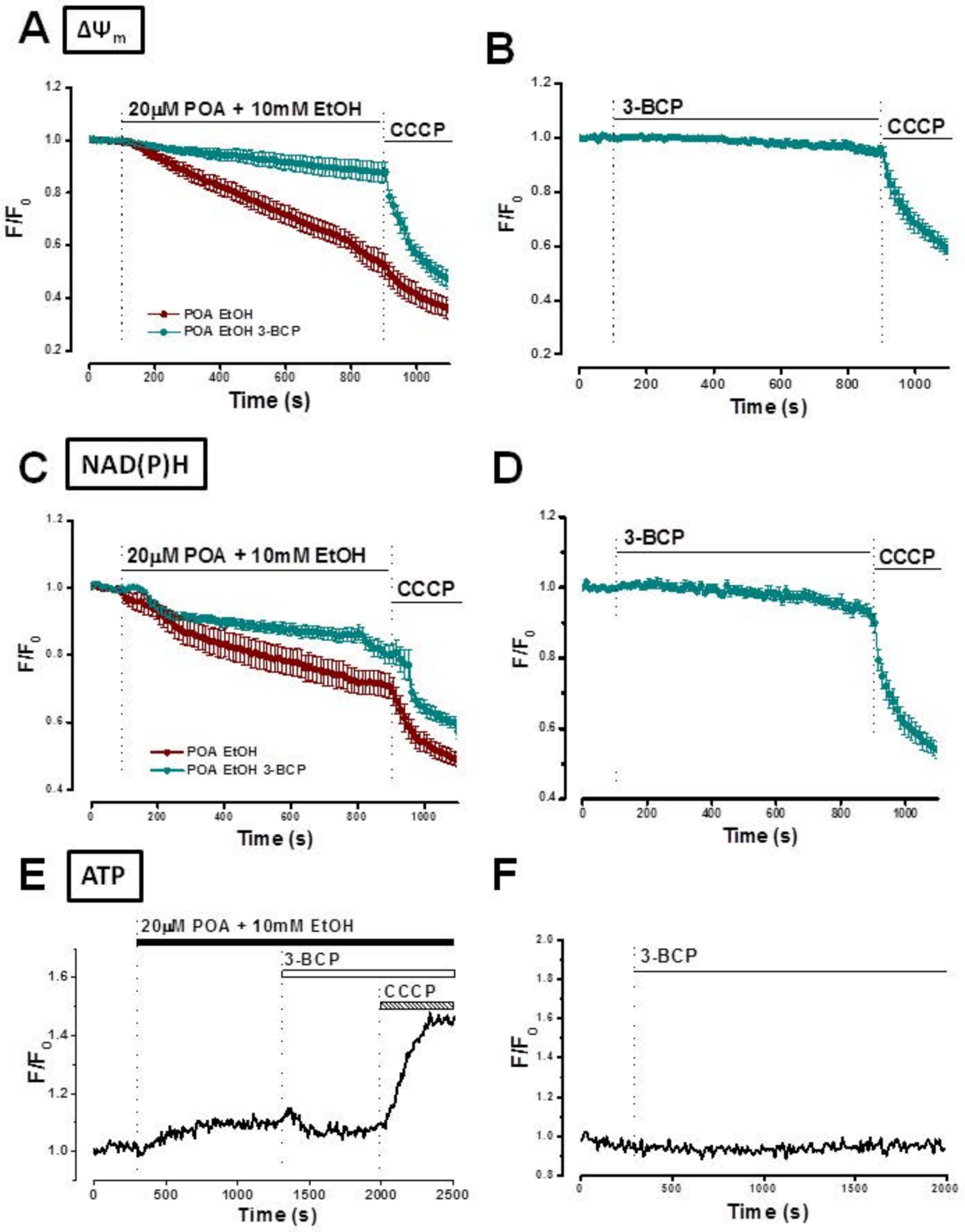
A
ΔΨm
20μM POA + 10mM EtOH
CCCP
POA EtOH
POA EtOH 3-BCP
F/F0
Time (s)
B
3-BCP
CCCP
F/F0
Time (s)
C
NAD(P)H
20μM POA + 10mM EtOH
CCCP
POA EtOH
POA EtOH 3-BCP
F/F0
Time (s)
D
3-BCP
CCCP
F/F0
Time (s)
E
ATP
20μM POA + 10mM EtOH
3-BCP
CCCP
F/F0
Time (s)
F
3-BCP
F/F0
Time (s)